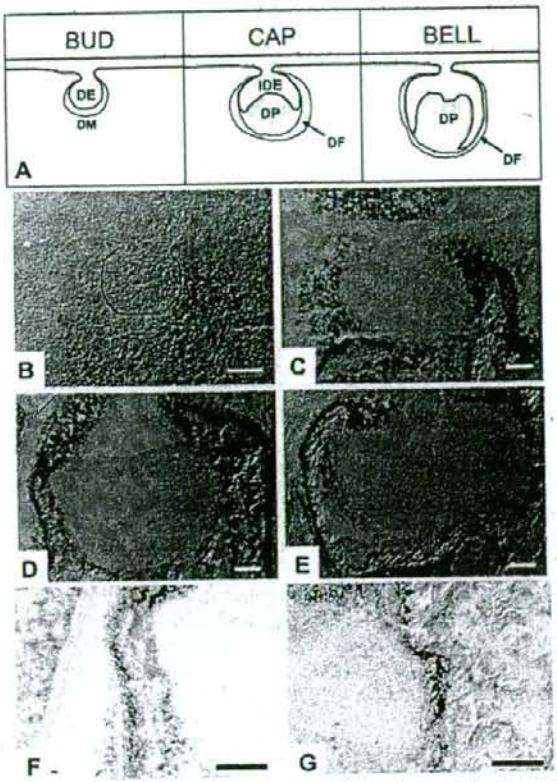

FIGURE 3. ***PLAP-1/asporin* expression in tooth development.** *A*, schematic representation of molar tooth development. *DE*, dental epithelium; *DM*, dental mesenchyme; *IDE*, inner enamel epithelium; *DP*, dental papilla; *DF*, dental follicle. *B–G*, *in situ* hybridization of *PLAP-1/asporin* in tooth germ at different stages of development. *B*, no expression at the bud stage (E13). The *black line* shows an outline of the tooth germ. *C*, restricted expression to the dental follicle at the cap stage (E15.5). *D*, early bell stage (E18). *E*, late bell stage (postnatal day 1). There is continuous expression of *PLAP-1/asporin* in dental follicle throughout the early and late bell stages. *F*, higher magnification of *D*. *G*, higher magnification of *E*. *Scale bars*, 100 μm.

Among the cell lines, one cell line, designated MPDL22, showed the highest ALPase activity and formed calcified nodules during culture. Thus, we selected MPDL22 for further characterization.

We assessed the expression of mineralized tissue-related genes in MPDL22 (Fig. 5). We cultured various cell clones in the mineralization medium for 8 days and then performed RT-PCR analysis. MPDL22 cells were positive for various extracellular matrix genes, collagen type I, collagen type III, collagen type XII, periostin, *PLAP-1/asporin*, and osteopontin (Fig. 5*B*). In terms of osteoblastic transcriptional factors, MPDL22 cells were positive for *Runx2*, *Msx2*, *Dlx5*, and Osterix (Fig. 5*A*). MG/B6 cells, derived from mouse gingival connective tissues, were also cultured in the mineralization medium. As expected, MG/B6 showed no ALPase activity even when the cells were cultured in the mineralization medium. Moreover MG/B6 demonstrated no expression of osteoblastic transcriptional factors and collagen type XII, periostin, and *PLAP-1/asporin*. We concluded that MPDL22 had a high potential for mineralization and could be a progenitor of osteoblasts or cementoblasts. In this study, we used MPDL22 as host cells for further investigation.

Overexpression of PLAP-1/Asporin in MPDL22 Suppresses Cytodifferentiation and Mineralization—To explore the role of PLAP-1/asporin in PDL cell cytodifferentiation and mineralization, we established MPDL22 cells overexpressing PLAP-1/asporin. We transfected the MPDL22 cells with the vector expressing PLAP-1/asporin. After drug selection, we established stable transfectants that were overexpressing PLAP-1/asporin (Fig. 6*A*). We cultured the transfected cells in mineralization medium and measured ALPase activity (Fig. 6*B*). ALPase activity of the transfectants overexpressing PLAP-1/asporin was significantly suppressed during culture compared with the ALPase activity of mock-transfected control MPDL22 cells (Fig. 6*B*). Alizarin red S staining of the transfectants on days 12 and 15 of culture revealed that calcified nodule formation of the transfectant overexpressing PLAP-1/asporin was suppressed compared with that of mock-transfected control MPDL22 cells (Fig. 6*C*). These results suggest that PLAP-1/asporin may negatively regulate PDL cell mineralization.

PLAP-1/Asporin Regulates BMP-2-induced Cytodifferentiation of MPDL22—BMP-2 is one of the most potent cytokines that stimulates osteoblast differentiation and bone formation (19). BMP-2 has also been reported to stimulate osteoblastic differentiation of human PDL cells (20) and to promote dental follicle cells that are putative progenitor cells for the periodontium that differentiate into a cementoblastic/osteoblastic phenotype (21). As expected, BMP-2 enhanced the ALPase activity and the calcified nodule

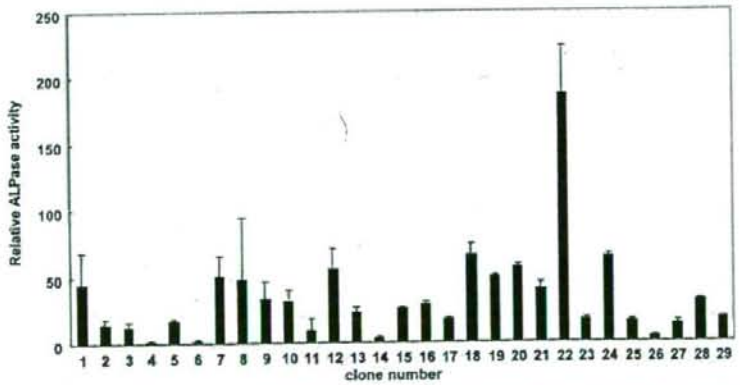

FIGURE 4. **ALPase activities of mouse PDL cell clones after 8 days in the mineralization medium.** Results are presented as the ratio of ALPase activity of each clone to clone number 4 (MPDL4). Clone number 22 (MPDL22) showed the highest ALPase activity. The values are given as means ± S.D. of triplicate assays. For reference, the ratio of ALPase activity of MG/B6 (see Fig. 5), which was derived from mouse gingival connective tissues, was 0.18 ± 0.34.

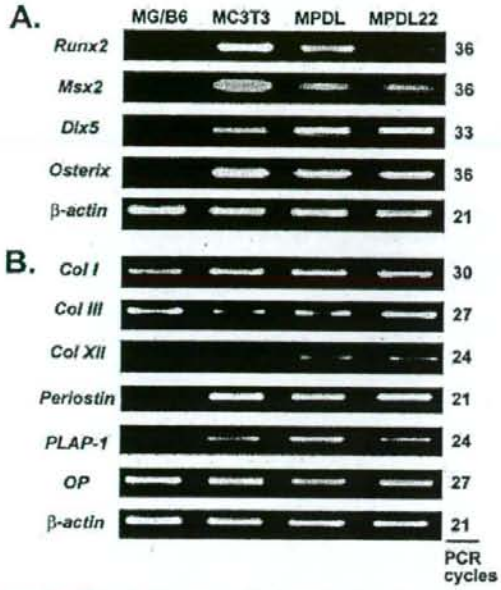

FIGURE 5. **RT-PCR analysis of genes related to mineralized tissue in MPDL22.** *A*, transcriptional factors. MPDL22 showed positive expression of *Runx2*, *Msx2*, *Dlx5*, and Osterix, which are osteoblastic transcriptional factors. MG/B6, a mouse gingival fibroblast cell clone, showed no expression of osteoblastic transcriptional factors. *B*, extracellular matrix genes. MPDL22 expressed all of the extracellular matrix transcripts that were analyzed. MC3T3-E1 showed weak expression of collagen (*Col*) type III and type XII. *OP*, osteopontin.

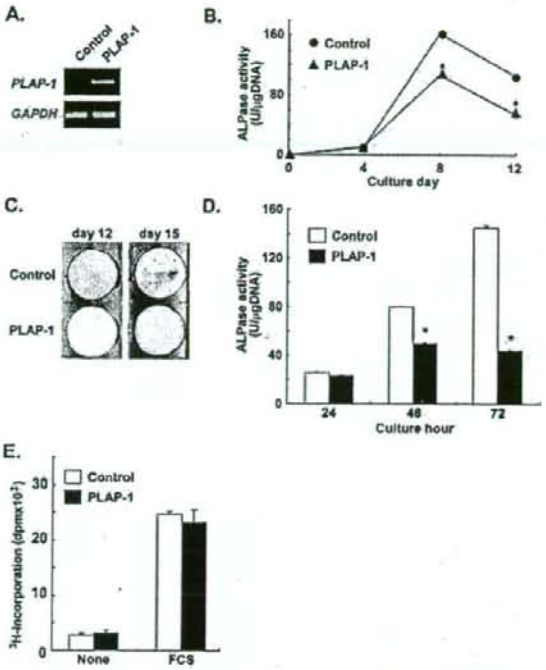

FIGURE 6. **Overexpression of PLAP-1/asporin in MPDL22 suppresses cytodifferentiation and mineralization.** *A*, RT-PCR analysis of *PLAP-1/asporin* expression in the transfected MPDL22 cells. *B*, PLAP-1/asporin inhibits ALPase activities. The values are given as means ± S.D. of triplicate assays. *, $p < 0.05$. *C*, PLAP-1/asporin suppresses calcified nodule formation. Alizarin red staining was performed after culture in mineralization medium for 12 and 15 days. *D*, PLAP-1/asporin inhibits BMP-2-induced ALPase activities. Shown are ALPase activities after stimulation by BMP-2 (100 ng/ml) for the indicated hours. The values are given as means ± S.D. of triplicate assays. *, $p < 0.05$. *E*, PLAP-1/asporin does not suppress proliferation activities. Shown is [^{3}H]thymidine incorporation of the transfected MPDL22 cells after stimulation by 10% FCS. The values are given as means ± S.D. of triplicate assays. Representative results of three independent experiments are shown. *GAPDH*, glyceraldehyde-3-phosphate dehydrogenase; *U*, units.

formation of MPDL22 cells (data not shown). On the other hand, in human PDL cells, *PLAP-1/asporin* transcript was regulated by BMP-2, and BMP-2 stimulation of human PDL cells up-regulated PLAP-1/asporin expression (9). Given that BMP-2 induced PDL cell cytodifferentiation and mineralization, we speculated that PLAP-1/asporin could negatively regulate PDL cell cytodifferentiation and mineralization through BMP-2. Thus, we examined the effects of overexpressing PLAP-1/asporin on BMP-2-induced MPDL cell cytodifferentiation (Fig. 6*D*). BMP-2 induced ALPase activity of the mock-transfected control MPDL22 cells. On the other hand, BMP-2-induced ALPase activity in the transfectants overexpressing PLAP-1/asporin was significantly inhibited. These results suggest that PLAP-1/asporin negatively regulates MPDL22 cell cytodifferentiation and mineralization through BMP-2 functions. Furthermore we assessed whether or not the effect of PLAP-1/asporin overexpression could be general suppression of cellular activities. We stimulated the transfectant cells with 10% FCS and assessed the proliferation activities (Fig. 6*E*). The transfectant cells overexpressing PLAP-1/asporin showed proliferation activity equivalent to the mock-transfected control cells by FCS stimulation. These results reveal that overexpression of PLAP-1/asporin does not result in general suppression of the cellular activity.

To examine the effects of PLAP-1/asporin knockdown on BMP-2-induced cytodifferentiation, we established MPDL transfectant cells that had shRNA introduced for the *PLAP-1/asporin* gene. We designed two different shRNA sequences specific for *PLAP-1/asporin* mRNA and constructed two independent shRNA expression plasmids. We obtained two different transfectant cell lines by stably transfecting the MPDL22 cells with each plasmid independently. These cell lines showed reduced *PLAP-1/asporin* transcript expression (Fig. 7*A*). One transfectant cell line, 326i, showed complete reduction of the *PLAP-1/asporin* transcript. On the other hand, 1260i showed a partial reduction of the transcript. To assess the effects of *PLAP-1/asporin* RNA interference on BMP-2-induced ALPase activity, we assayed the activity of ALPase on BMP-2 stimulation (Fig. 7*B*). 326i showed significant hyper-responsiveness to BMP-2 stimulation; 1260i also showed significant enhancement of ALPase activity. However, consistent with the reduced *PLAP-1/asporin* transcript level, the enhancement of ALPase activity in 1260i was lower than that in 326i. We then assayed BMP-2-induced gene expression by RT-PCR analysis (Fig. 7*C*). 326i and 1260i showed strong induction of BMP-2-induced bone sialoprotein and osteocalcin expression compared with con-

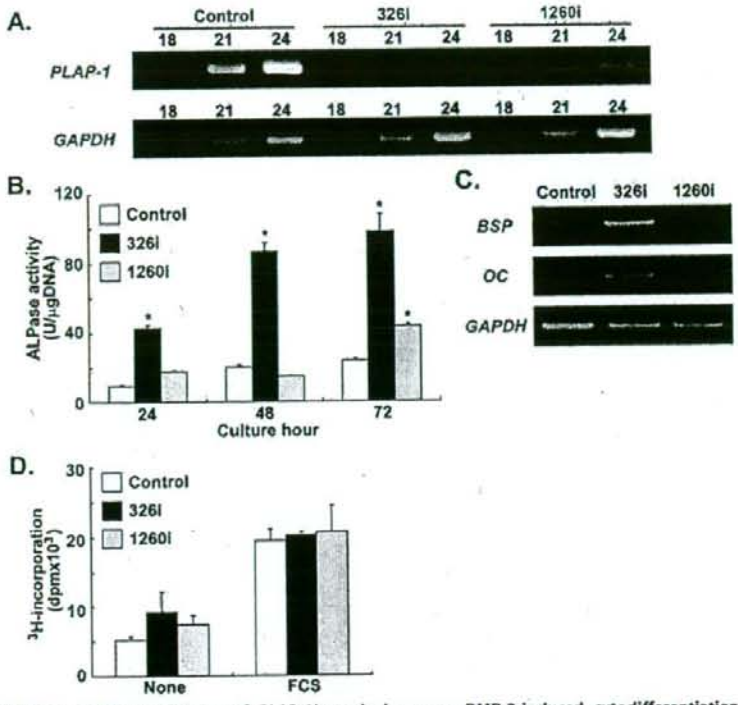

FIGURE 7. **Stable knockdown of *PLAP-1/asporin* increases BMP-2-induced cytodifferentiation of MPDL22.** *A*, steady-state levels of *PLAP-1/asporin* in MPDL22 cells. RT-PCR analysis of *PLAP-1/asporin* was carried out. The number of PCR cycles is shown *above* each *lane*. *Control*, MPDL22 stably transfected with an expression vector for control shRNA; *326i*, MPDL22 stably transfected with an expression vector for *PLAP-1/asporin* shRNA in target site 326; *1260i*, MPDL22 stably transfected with an expression vector for *PLAP-1/asporin* shRNA in target site 1260. *B*, increased response to BMP-2 following knockdown of *PLAP-1/asporin*. MPDL22 cells stably transfected with control or *PLAP-1/asporin* shRNA expression vector were treated with 100 ng/ml BMP-2. ALPase activities of the transfectants were assayed after BMP-2 stimulation for 24, 48, and 72 h. The values are given as means ± S.D. of triplicate assays. *, $p < 0.05$. *C*, strong induction of BMP-2-induced gene expression in *PLAP-1/asporin* shRNA transfectants. RT-PCR analysis was performed after BMP-2 stimulation for 48 h. The number of PCR cycles was 33, 30, and 22 for bone sialoprotein (*BSP*), osteocalcin (*OC*), and glyceraldehyde-3-phosphate dehydrogenase (*GAPDH*), respectively. *D*, RNA interference of *PLAP-1/asporin* does not suppress proliferation activities. Shown is [³H]thymidine incorporation of the shRNA-transfected MPDL22 cells after stimulation by 10% FCS. The values are given as means ± S.D. of triplicate assays. Representative results of three independent experiments are shown. *U*, units.

trol cells. The enhancement of bone sialoprotein and osteocalcin gene expression in 1260i was also lower than that in 326i, consistent with the reduced *PLAP-1/asporin* transcript level. Then we assessed whether or not RNA interference of *PLAP-1/asporin* could affect the general cellular activity. We stimulated the shRNA transfectant cells with 10% FCS and assessed the proliferation activities (Fig. 7*D*). 326i and 1260i cells showed proliferation activity equivalent to the control cells by FCS stimulation. These results indicate that RNA interference of *PLAP-1/asporin* does not affect the general cellular activity.

PLAP-1/Asporin Binds to BMP-2 in Vitro—It has been reported that other SLRP family proteins (including decorin, biglycan, and PLAP-1/asporin) bind to TGF-β1 (10, 22). In addition, biglycan binds to BMP-4 (23). These observations suggest the possibility that PLAP-1/asporin can also interact with BMP-2. We investigated this possibility by testing the ability of recombinant PLAP-1/asporin protein to bind BMP-2 (Fig. 8). First we confirmed the purity of silkworm-derived recombinant His-tagged PLAP-1/asporin protein by SDS-PAGE and Western blot analysis using anti-His antibody (Fig. 8*A*). Recombinant PLAP-1/asporin protein was detected at around 43 kDa, which is the expected molecular mass of PLAP-1/asporin protein (7) by SDS-PAGE and Western blot analysis under the reduced condition. We then performed immunoprecipitation experiments using the recombinant His-tagged PLAP-1/asporin protein and BMP-2 (Fig. 8*B*). We found that PLAP-1/asporin co-precipitated with BMP-2 (Fig. 8*B*, *lane 2*). Reciprocal co-immunoprecipitation experiments also showed that PLAP-1/asporin can be found in the BMP-2 precipitate (Fig. 8*B*, *lane 4*). These results confirm the direct *in vitro* interaction between PLAP-1/asporin and BMP-2.

Co-localization of PLAP-1/Asporin and BMP-2 in MPDL22 Cells—To further understand the relationship between PLAP-1/asporin and BMP-2 binding at a cellular level, we performed two-color immunohistochemical staining of FLAG-tagged PLAP-1/asporin-transfected MPDL22 cells, which were preincubated with BMP-2 using anti-FLAG and anti-BMP-2 antibodies (Fig. 7). The co-localization of PLAP-1/asporin (*green*) and BMP-2 (*red*) were detected coincidentally in the FLAG-tagged PLAP-1/asporin-transfected MPDL22 cells, shown in the *orange* staining (Fig. 9*F*). This shows that PLAP-1/asporin and BMP-2 can bind at a cellular level. Interestingly the FLAG-tagged PLAP-1/asporin-transfected MPDL22 cells show more BMP-2 binding than mock-transfected control MPDL22 cells. This suggests that PLAP-1/asporin could control BMP-2 binding at the cellular level.

DISCUSSION

In this study, we have described the localization and potential function of PLAP-1/asporin. Our data demonstrate that *PLAP-1/asporin* is a PDL-specific gene that negatively regulates PDL cell cytodifferentiation and mineralization. The localization of PLAP-1/asporin is unique. The similar localization is not found with any other member of the small leucine-rich repeat proteoglycan family. We recently reported that the expression of PLAP-1/asporin is tightly regulated by BMP-2, one of the

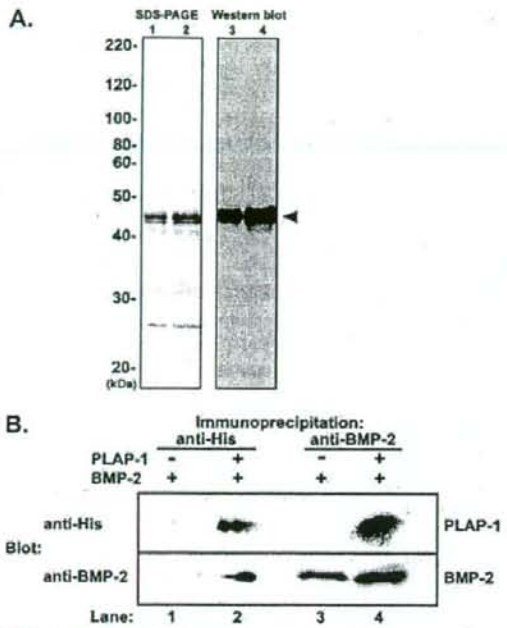

FIGURE 8. **PLAP-1/asporin binds to BMP-2 *in vitro*.** *A*, SDS-PAGE and Western blot analysis of the recombinant PLAP-1/asporin. Purified silkworm-derived His-tagged PLAP-1/asporin protein was analyzed by SDS-PAGE and Western blotting under reduced condition. The SDS-PAGE gel was stained with silver staining. His-tagged PLAP-1/asporin was detected with anti-polyhistidine antibody in Western blotting. *Lanes 1* and *3*, 0.3 μg of recombinant PLAP-1/asporin was applied. *Lane 2* and *4*, 0.6 μg of recombinant PLAP-1/asporin was applied. The *arrowhead* indicates recombinant PLAP-1/asporin protein. Positions of molecular mass markers are shown on the *left side*. *B*, recombinant BMP-2 was incubated with or without His-tagged PLAP-1/asporin. Immunoprecipitation using anti-polyhistidine antibody was carried out (*lanes 1* and *2*). Co-precipitated His-tagged PLAP-1/asporin was detected with anti-polyhistidine antibody (*upper panel*), and BMP-2 was detected with anti-BMP-2 antibody (*lower panel*). Reverse immunoprecipitation using anti-BMP-2 antibody was carried out (*lanes 3* and *4*) followed by Western blotting with anti-polyhistidine antibody (*upper panel*) or anti-BMP-2 antibody (*lower panel*).

most potent cytokines for mineralization (9). This study demonstrates that PLAP-1/asporin regulates PDL cell cytodifferentiation through BMP-2 activity, which suggests that PLAP-1/asporin is part of the negative feedback mechanism of BMP-2.

We showed that, in the adult mouse, *PLAP-1/asporin* is preferentially expressed in the periodontal ligament. The PDL is a highly vascular and cellular connective tissue that plays critical roles in mineralized tissue generation and support. The periodontal ligament is situated between the tooth and the alveolar bone, and it supports the attachment of the teeth to the alveolar bone. Furthermore mesenchymal stem cells are present in the PDL and are able to differentiate into multiple types of cells that play essential roles by responding to the mechanical forces that affect teeth and by repairing damaged matrix (24). Preferential localization of *PLAP-1/asporin* in the PDL suggests that it has different and unique roles in the homeostasis and function of the PDL.

The *in situ* hybridization analysis of *PLAP-1/asporin* in mouse embryogenesis revealed that, in the maxilla and mandible, the first expression was detected at E12.5; this was followed at E13.5 by *PLAP-1/asporin* expression in the mesenchyme lateral to Meckel cartilage (8). In the present study, we showed that *PLAP-1/asporin* expression is markedly enhanced in dental follicle cells of the developing tooth germ. During tooth germ development, progenitor cells present in the dental follicle are believed to play a central role in the formation of periodontal components such as cementum, periodontal ligament, and alveolar bone (25, 26). Taken together, PLAP-1/asporin appears to be involved in the formation of periodontal tissues during tooth development.

In this study, we established a PDL cell clone to analyze PLAP-1/asporin functions *in vitro*. PDL cells have been reported to be osteogenic in nature and to differentiate into either osteoblasts or cementoblasts depending on the need and the environment. *In vitro* maintained PDL cells obtained from rats formed mineralized nodules that were different from those formed by osteoblasts (4). It has also been shown that human PDL cells, but not gingival fibroblasts, form mineral-like nodules *in vitro* (5). However, in most of the previous studies, the PDL cells were heterogeneous cell populations. Thus, it was difficult to clarify which of the cells, alone or interacting with other cell types, were responsible for the calcified nodule formation. Our findings, obtained using PDL cell clones, further indicate that PDL cells are closely related to the osteogenic cell lineage because PDL clone cells were shown to express genes, including *Runx2*, thought to be specific to osteoblasts and to produce mineralized nodules during the cytodifferentiation process.

By using the PDL cell clones, we demonstrated that PLAP-1/asporin represses the cytodifferentiation and mineralization that occurs during the PDL differentiation process. We also found that PLAP-1/asporin negatively regulates the BMP-2-induced differentiation of PDL cells. Interestingly we demonstrated that recombinant PLAP-1/asporin directly interacts with BMP-2 *in vitro*. We also found that recombinant PLAP-1/asporin inhibits the BMP-2-induced differentiation of PDL cells (72.8% inhibition to control). These findings are supported by the previous report showing that PLAP-1/asporin suppresses chondrogenesis by inhibiting TGF-β function through a direct interaction (10). Both BMP-2 and TGF-β belong to the TGF-β superfamily and share consensus structures. TGF-β signaling is crucial for maintaining articular cartilage and for preventing osteoarthritis. On the other hand, BMP-2 plays crucial roles in bone formation and metabolism. Our findings strongly suggest that PLAP-1/asporin binds directly to BMP-2 and suppresses BMP-2 signaling in PDL tissues *in vivo*. The actual binding site of PLAP-1/asporin to BMP-2 is still unclear. However, there are some reports showing that leucine-rich repeats (LRRs), which are found in PLAP-1/asporin, are involved in protein-protein interactions and have been found in a large number of proteins, including SLRP family proteins such as decorin, biglycan, fibromodulin, and lumican (27). Decorin binds to collagen mainly through LRR-4 and -5 of the core protein (28). In addition, a high affinity binding site for TGF-β is located between LRR-3 and -5 (29).

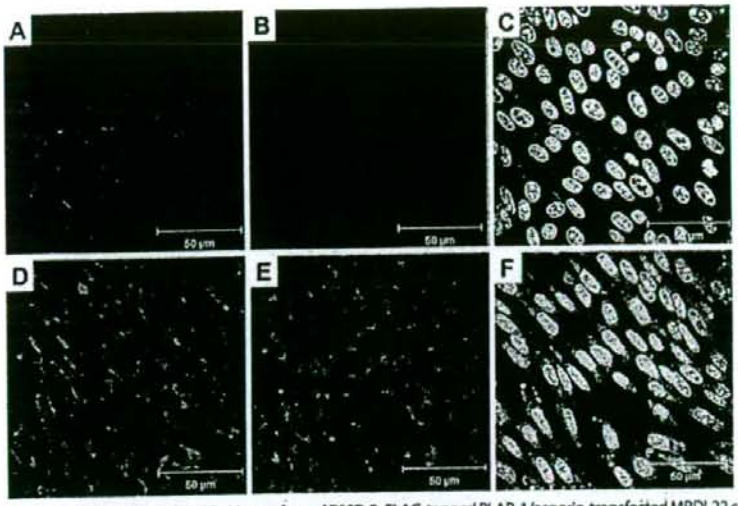

FIGURE 9. **Co-localization of PLAP-1/asporin and BMP-2.** FLAG-tagged PLAP-1/asporin-transfected MPDL22 cells were analyzed by two-color immunohistochemical staining. Transfected cells were preincubated with BMP-2 (10 μg/ml) before staining. *A–C*, mock-transfected control MPDL22 cells. *D–F*, FLAG-tagged PLAP-1/asporin-transfected MPDL22 cells. *A* and *D*, anti-BMP-2 staining (*red*). *B* and *E*, anti-FLAG staining (*green*). *C* and *F*, merged image of anti-BMP-2 and anti-FLAG staining. Nuclear staining with 4′,6-diamidino-2-phenylindole is shown in *blue*.

Decorin binding to TGF-β prevents the binding of TGF-β to its receptor and regulates TGF-β-mediated cellular signaling (30). It is also suggested that decorin interacts with vascular endothelial growth factor through LRR-5 (31). Taken together, it is quite possible that PLAP-1/asporin interacts with BMP-2 through LRRs, and we are currently conducting experiments to assess this possibility.

Decorin and biglycan show high homology and similarity to PLAP-1/asporin (6–8). Interestingly recent studies have revealed that biglycan positively modulates osteoblast differentiation and matrix mineralization by regulating BMP-4 signaling (23, 32). On the other hand, decorin has been shown to suppress osteoblast differentiation *in vitro* (33). In our study, the overexpression of PLAP-1/asporin in MC3T3-E1 preosteoblastic cells was found to inhibit osteoblast differentiation and mineralization (data not shown). These opposing effects of SLRPs on osteoblast differentiation and mineralization have not been explained. The three SLRPs have different numbers of glycosaminoglycan attachment sites. PLAP-1/asporin has no glycosaminoglycan site, whereas biglycan has two glycosaminoglycan sites, and decorin has one glycosaminoglycan site (6–8). These differences may contribute to the specific functions that the various SLRPs have in cytodifferentiation and mineralization.

Ankylosis between tooth root and alveolar bone results in pathological resorption of the tooth and bone, leading to fracture. As cited above, the PDL has a high osteogenic potential, and many PDL cells highly express Runx2 and ALPase *in vivo* (34). However, the PDL is comprised of tough yet flexible connective tissue *in vivo*. The molecular mechanism by which the PDL is maintained and not ossified has not yet been fully clarified. Msx2, which is a transcriptional factor with a homeobox domain, has recently been reported to be dominantly expressed in the PDL and to suppress PDL cytodifferentiation and mineralization through the inhibition of Runx2 functions (35). Another study revealed that S100A4, which is an intracellular calcium-binding protein, suppresses differentiation of PDL cells as well as osteoblasts (36, 37). However, the expression of these molecules is relatively ubiquitous. In contrast, *PLAP-1/asporin* showed very specific expression in limited tissue types. This supports the idea that PLAP-1/asporin, compared with other molecules, has other functions in the PDL in addition to regulating PDL cell differentiation.

In conclusion, we showed that endogenous PLAP-1/asporin may prevent the PDL from undergoing osteogenic and cementogenic processes probably by inhibiting BMP-2 functions to maintain PDL homeostasis *in vivo*. This may be the molecular mechanism by which the PDL prevents the onset of ossification despite having osteoblastic potential.

REFERENCES

1. Beertsen, W., McCulloch, C. A., and Sodek, J. (1997) *Periodontol. 2000* **13,** 20–40
2. Bartold, P. M., Shi, S., and Gronthos, S. (2006) *Periodontol. 2000* **40,** 164–172
3. Seo, B. M., Miura, M., Gronthos, S., Bartold, P. M., Batouli, S., Brahim, J., Young, M., Robey, P. G., Wang, C. Y., and Shi, S. (2004) *Lancet* **364,** 149–155
4. Cho, M. I., Matsuda, N., Lin, W. L., Moshier, A., and Ramakrishnan, P. R. (1992) *Calcif. Tissue Int.* **50,** 459–467
5. Arceo, N., Sauk, J. J., Moehring, J., Foster, R. A., and Somerman, M. J. (1991) *J. Periodontol.* **62,** 499–503
6. Yamada, S., Murakami, S., Matoba, R., Ozawa, Y., Yokokoji, T., Nakahira, Y., Ikezawa, K., Takayama, S., Matsubara, K., and Okada, H. (2001) *Gene (Amst.)* **275,** 279–286
7. Lorenzo, P., Aspberg, A., Onnerfjord, P., Bayliss, M. T., Neame, P. J., and Heinegard, D. (2001) *J. Biol. Chem.* **276,** 12201–12211
8. Henry, S. P., Takanosu, M., Boyd, T. C., Mayne, P. M., Eberspaecher, H., Zhou, W., de Crombrugghe, B., Hook, M., and Mayne, R. (2001) *J. Biol. Chem.* **276,** 12212–12221
9. Yamada, S., Ozawa, Y., Tomoeda, M., Matoba, R., Matsubara, K., and Murakami, S. (2006) *J. Dent. Res.* **85,** 447–451
10. Kizawa, H., Kou, I., Iida, A., Sudo, A., Miyamoto, Y., Fukuda, A., Mabuchi, A., Kotani, A., Kawakami, A., Yamamoto, S., Uchida, A., Nakamura, K., Notoya, K., Nakamura, Y., and Ikegawa, S. (2005) *Nat. Genet.* **37,** 138–144
11. Iida, A., Kizawa, H., Nakamura, Y., and Ikegawa, S. (2006) *J. Hum. Genet.* **51,** 151–154
12. Ikegawa, S., Kawamura, S., Takahashi, A., Nakamura, T., and Kamatani, N. (2006) *Arthritis Res. Ther.* **8,** 403
13. Toyosawa, S., Shintani, S., Fujiwara, T., Ooshima, T., Sato, A., Ijuhin, N., and Komori, T. (2001) *J. Bone Miner. Res.* **16,** 2017–2026
14. Reynolds, A., Leake, D., Boese, Q., Scaringe, S., Marshall, W. S., and Khvorova, A. (2004) *Nat. Biotechnol.* **22,** 326–330
15. Bessey, O., Lowry, O., and Brock, M. (1946) *J. Biol. Chem.* **164,** 321–329
16. Dahl, L. K. (1952) *Proc. Soc. Exp. Biol. Med.* **80,** 474–479
17. Labarca, C., and Paigen, K. (1980) *Anal. Biochem.* **102,** 344–352

18. Ishihara, K., Satoh, I., Nittoh, T., Kanaya, T., Okazaki, H., Suzuki, T., Koyama, T., Sakamoto, T., Ide, T., and Ohuchi, K. (1999) *Biochim. Biophys. Acta* **1451,** 48–58
19. Hogan, B. L. (1996) *Curr. Opin. Genet. Dev.* **6,** 432–438
20. Kobayashi, M., Takiguchi, T., Suzuki, R., Yamaguchi, A., Deguchi, K., Shionome, M., Miyazawa, Y., Nishihara, T., Nagumo, M., and Hasegawa, K. (1999) *J. Dent. Res.* **78,** 1624–1633
21. Zhao, M., Xiao, G., Berry, J. E., Franceschi, R. T., Reddi, A., and Somerman, M. J. (2002) *J. Bone Miner. Res.* **17,** 1441–1451
22. Hildebrand, A., Romaris, M., Rasmussen, L. M., Heinegard, D., Twardzik, D. R., Border, W. A., and Ruoslahti, E. (1994) *Biochem. J.* **302,** 527–534
23. Chen, X. D., Fisher, L. W., Robey, P. G., and Young, M. F. (2004) *FASEB J.* **18,** 948–958
24. Lekic, P., and McCulloch, C. A. (1996) *Anat. Rec.* **245,** 327–341
25. Bosshardt, D. D., and Schroeder, H. E. (1996) *Anat. Rec.* **245,** 267–292
26. Saito, M., Handa, K., Kiyono, T., Hattori, S., Yokoi, T., Tsubakimoto, T., Harada, H., Noguchi, T., Toyoda, M., Sato, S., and Teranaka, T. (2005) *J. Bone Miner. Res.* **20,** 50–57
27. Matsushima, N., Ohyanagi, T., Tanaka, T., and Kretsinger, R. H. (2000) *Proteins* **38,** 210–225
28. Svensson, L., Heinegard, D., and Oldberg, A. (1995) *J. Biol. Chem.* **270,** 20712–20716
29. Schonherr, E., Broszat, M., Brandan, E., Bruckner, P., and Kresse, H. (1998) *Arch. Biochem. Biophys.* **355,** 241–248
30. Stander, M., Naumann, U., Wick, W., and Weller, M. (1999) *Cell Tissue Res.* **296,** 221–227
31. Sulochana, K. N., Fan, H., Jois, S., Subramanian, V., Sun, F., Kini, R. M., and Ge, R. (2005) *J. Biol. Chem.* **280,** 27935–27948
32. Parisuthiman, D., Mochida, Y., Duarte, W. R., and Yamauchi, M. (2005) *J. Bone Miner. Res.* **20,** 1878–1886
33. Mochida, Y., Duarte, W. R., Tanzawa, H., Paschalis, E. P., and Yamauchi, M. (2003) *Biochem. Biophys. Res. Commun.* **305,** 6–9
34. Saito, Y., Yoshizawa, T., Takizawa, F., Ikegame, M., Ishibashi, O., Okuda, K., Hara, K., Ishibashi, K., Obinata, M., and Kawashima, H. (2002) *J. Cell Sci.* **115,** 4191–4200
35. Yoshizawa, T., Takizawa, F., Iizawa, F., Ishibashi, O., Kawashima, H., Matsuda, A., Endo, N., and Kawashima, H. (2004) *Mol. Cell. Biol.* **24,** 3460–3472
36. Duarte, W. R., Shibata, T., Takenaga, K., Takahashi, E., Kubota, K., Ohya, K., Ishikawa, I., Yamauchi, M., and Kasugai, S. (2003) *J. Bone Miner. Res.* **18,** 493–501
37. Duarte, W. R., Iimura, T., Takenaga, K., Ohya, K., Ishikawa, I., and Kasugai, S. (1999) *Biochem. Biophys. Res. Commun.* **255,** 416–420

Available online at www.sciencedirect.com
ScienceDirect
Matrix Biology 27 (2008) 232–241
MATRIX BIOLOGY
www.elsevier.com/locate/matbio

Basic fibroblast growth factor regulates expression of heparan sulfate in human periodontal ligament cells

Yoshio Shimabukuro, Tomoo Ichikawa, Yoshimitsu Terashima, Tomoaki Iwayama, Hiroyuki Oohara, Tetsuhiro Kajikawa, Ryohei Kobayashi, Hiroaki Terashima, Masahide Takedachi, Mami Terakura, Tomoko Hashikawa, Satoru Yamada, Shinya Murakami *

Department of Periodontology, Division of Oral Biology and Disease Control, Osaka University Graduate School of Dentistry, 1-8 Yamadaoka, Suita, Osaka 565-0871, Japan

Received 30 March 2006; received in revised form 25 September 2007; accepted 19 October 2007

Abstract

Heparan sulfate (HS) proteoglycan is a widely distributed biological molecule that mediates a variety of physiological responses in development, cell growth, cell migration, and wound healing. We examined the effects of basic fibroblast growth factor-2 (FGF-2), which is known to modulate extracellular matrix (ECM) production of various cell types, on the production of HS proteoglycan by human periodontal ligament (HPDL) cells. We also examined the effects of FGF-2 on the expression of syndecans, a major family of membrane-bound HS proteoglycans. Treatment of HPDL cells with FGF-2 for 72 h resulted in a pronounced increase in the level of HS in the culture supernatant in a dose-dependent manner. However, reverse transcription-polymerase chain reaction data (RT-PCR) revealed that FGF-2 marginally reduced the gene expression of syndecan-1, -2, and -4, and did not alter the level of syndecan-3 mRNA. Furthermore, FGF-2 did not have an effect on the mRNA expression of enzymes associated with HS biosynthesis. Interestingly, FACS analysis revealed that the syndecan family displayed diverse alterations in response to FGF-2. FGF-2 barely altered the expression of syndecan-1, but decreased the expression of syndecan-2 and -4 on HPDL cells. Moreover, dot blot analysis showed that FGF-2 did not alter the level of syndecan-1 and -2, but enhanced the level of syndecan-4 in culture supernatants of FGF-2-stimulated HPDL cells. These results suggest that the FGF-2-activated increase in the level of HS in conditioned medium may be a result of shedding of syndecan-4 from the HPDL cell surface. Taken together, FGF-2 may differentially regulate the expression of HS proteoglycans in a HS-proteoglycan-subtype-dependent manner. The diversity of the expression patterns of HS proteoglycans may be associated with the FGF-2-induced biological functions of HPDL cells.

Keywords: Basic fibroblast growth factor; Heparan sulfate; Periodontal ligament cells; Shedding; Syndecan

1. Introduction

A wide range of extracellular matrix and growth factors participate during the wound-healing process. The basic fibroblast growth factor-2 (FGF-2) is one such growth factor detected in the early phase of wound healing. FGF-2 mediates various biological responses including cellular proliferation, angiogenesis, and tissue repair (Bikfalvi et al., 1997; Nugent and Iozzo, 2000). FGF-2 also modulates the expression of glycosaminoglycans and proteoglycans, as well as collagen and non-collagenous protein, which are main components of connective tissue. However, the details of the regulatory effects of FGF-2 on the expression of glycosaminoglycans and proteoglycans in cells have not been fully defined.

The syndecans are a family of cell surface heparan sulfate (HS) proteoglycans which comprise of a core protein and glycosaminoglycan side chains. Four members of the syndecan family have been identified to date. Whereas syndecan-4 expression is ubiquitous, syndecan-1, -2, and -3 are mainly present in epithelial cells, fibroblasts, and neural cells, respectively. The HS chains of the syndecans are responsible for their biological

* Corresponding author. Tel.: +81 6 6879 2930; fax: +81 6 6879 2934.
E-mail address: ipshinya@dent.osaka-u.ac.jp (S. Murakami).

0945-053X/$ - see front matter © 2007 Elsevier B.V./International Society of Matrix Biology. All rights reserved.
doi:10.1016/j.matbio.2007.10.005

functions, such as extracellular matrix assembly and growth factor binding. The HS chains of syndecans are also known to function as co-receptors of the FGF receptor. It has been reported that when tissue was injured, syndecan expression was increased in epithelial cells, endothelial cells, and fibroblasts (Elenius et al., 1997; Gallo et al., 1996), and shed syndecan ectodomain accumulated in wound fluid (Fitzgerald et al., 2000; Kainulainen et al., 1998; Park et al., 2000). Recent studies have also revealed impaired wound healing in syndecan-deficient mice (Echtermeyer et al., 2001; Ishiguro et al., 2000; Stepp et al., 2002), suggesting an essential role for the syndecans in wound repair.

Periodontal tissue is a tooth-supporting tissue and consists of periodontal ligament, gingiva, cementum, and alveolar bone. The periodontal ligament cells have the potential to secrete a variety of extracellular matrices and support teeth with these molecules. Furthermore, they play key roles in regeneration events following periodontal tissue breakdown caused by progression of periodontal diseases. Interestingly, we revealed that topical application of FGF-2 to periodontal tissue defects activates regeneration of tissue with new cementum and ligament tissue formation (Murakami et al., 1999), which may be a result of FGF-2 increasing cell growth and modulating extracellular matrices. In addition, we explained the stimulatory effects of FGF-2 on the expression of the high molecular type of hyaluronan, a non-sulfated glycosaminoglycan, by human periodontal ligament (HPDL) cells via the up-regulation of hyaluronan synthase (HAS)1 and HAS2 (Shimabukuro et al., 2005). Here we examined the production of HS and the expression pattern of the syndecan gene family by HPDL cells in response to FGF-2.

2. Experimental procedures

2.1. Reagent

Human recombinant FGF-2 was provided by Kaken Pharmaceutical Co., Ltd. (Tokyo, Japan).

2.2. HPDL cells

HPDL cells were isolated from healthy periodontal ligaments of first premolar teeth of individuals undergoing tooth extraction for orthodontic treatment in accordance with the method of Somerman et al. (1988), with minor modifications. All the patients gave informed consent before providing the samples. Healthy periodontal tissue was removed from the center of the root surface with a surgical scalpel. The tissue was minced then transferred to Leighton tubes (Costor, Cambridge, MA, USA). The explants were cultured in α-MEM supplemented with 10% FCS, 50 U/ml penicillin G, and 50 μg/ml streptomycin (henceforth denoted standard medium), with medium changed every 2 or 3 days. Cells were cultured at 37 °C in a humidified atmosphere of 95% air and 5% CO_2. When the cells growing out from the explants had reached confluence, they were separated by treatment with a solution containing 0.05% trypsin and 0.53 mM ethylenediaminetetraacetic acid, collected by centrifugation, and cultured in standard medium in culture dishes until confluency. The cells were then trypsinized and split at a 1:3 ratio. Experiments were carried out with cells from the fourth to fifth passages. In this study, we established 3 cell lines from different volunteers, and all cell lines were used in each experiment. All these cell lines provided similar results in each experiment of this study.

2.3. Reverse transcription-polymerase chain reaction (RT-PCR) for quantitation of mRNA levels

HPDL cells were seeded at a density of 10^5 cells/dish in 600-mm dishes and grown to confluency in standard medium. Following 24 or 48 hours of activation in the absence or presence of FGF-2 (50 ng/ml), total RNA was isolated from HPDL cells by RNAzol™ (Cinna/Biotecx Laboratories Inc., Friendswood, TX, USA), according to the manufacturer's instructions. The precipitated RNA was resuspended in 0.1% diethylpyrocarbonate-treated distilled water (DEPC-treated H_2O). This RNA sample was heatdenatured at 65 °C for 10 min and chilled on ice. Complementary DNA (cDNA) synthesis and amplification via PCR were performed as described previously. cDNA synthesis was carried out in a 40 μl reverse transcription mixture containing 52.5 mM Tris–HCl; pH 8.3, 75.5 mM KCl, 3 mM $MgCl_2$, 0.5 mM each dNTPs, 1 mM dithiothreitol, 1.1 U/μl RNase inhibitor (Takara Biomedicals, Shiga, Japan), 55 ng/μl random hexamer, 5 U/μl M-MLV reverse transcriptase (Gibco, Gaithersburg, MD, USA) and RNA. The mixture was incubated at 37 °C for 60 min. At the end of the reverse transcription, all samples were heated at 99 °C for 5 min to inactivate the enzyme and were diluted into 110 μl of DEPC-treated H_2O.

Oligonucleotide PCR primers specific for HS biosynthesis-related enzymes, syndecan-1, -2, -3, and -4, and hypoxanthine phosphoribosyl transferase (HPRT) were synthesized at Takara Shuzo Co. Ltd. (Table 1).

Table 1
Primers utilized for reverse transcription-polymerase chain reaction

Primers	Size		Sequence
HPRT	303 bp	Sense	5′CGAGATGTGATGAAGGAGATGGG3′
		Antisense	5′GCCTGACCAAGGAAAGCAAAGTC3′
GlcNAcT-1	546 bp	Sense	5′CTAAGCTGCAGGGAAATAAA3′
		Antisense	5′TTGCTGTCTGTTGTTTGAAG3′
HS2ST	443 bp	Sense	5′AGGATTTTATCATGGACACG3′
		Antisense	5′TCTTTCCTGTGCGATAGAGT3′
NDST-1	450 bp	Sense	5′ATCTTCTGCCTGTTCAGCGT3′
		Antisense	5′CTCATTGGCCTTGAAGAAGC3′
NDST-2	580 bp	Sense	5′CATGAAGGTGGCTGAGTTG3′
		Antisense	5′CGGATTAAGCAGCACTGTCA3′
Epimerase	624 bp	Sense	5′AGGTGGTTAGGTTGATTGCG3′
		Antisense	5′GCAGTTGATTGATGTGGGTG3′
Syndecan-1	472 bp	Sense	5′CTTTGAAACCTCGGGGAGAATAC3′
		Antisense	5′TCCAGGCAGAAGTCAGAGAAGCAG3′
Syndecan-2	395 bp	Sense	5′GGAGCTGATGAGGATGTAGA3′
		Antisense	5′CACTGGATGGTTTGCGTTCT3′
Syndecan-3	292 bp	Sense	5′GCTTCTTTTCCCTTTTACCCTCCGC3′
		Antisense	5′TGTTCCCCAACTTCTCTCTGCCAAG3′
Syndecan-4	245 bp	Sense	5′GGGCAGGAATCTGATGACTTTGAG3′
		Antisense	5′GCTGGACATTGACACCTTGTTGC3′

PCR was performed in a 50 μl mixture containing 5 μl of each sample of derived cDNA, 10 mM Tris–HCl; pH 8.3, 50 mM KCl, 1.5 mM $MgCl_2$, 0.15 mM of each dNTP, 1.25 mM Ampli Taq Gold™ (Perkin Elmer Cetus Co., Emeryville, CA, USA) and 0.2 mM of each primer. After 9 min of predenaturation at 94 °C, PCR was performed in a DNA thermal cycler (MJ Research Inc., Watham, MA, USA) for 21, 24, 27, 30, 33 and 36 cycles to optimize the cycle number to maintain exponential conditions of amplification. Each cycle consisted of denaturation at 94 °C for 45 s, annealing at 56 °C for 45 s, polymerization at 72 °C for 90 s. The 7 μl samples were analyzed on 2% agarose ethidium bromide gels run at 100 V for 25–30 min.

2.4. Determination of the level of HS in culture supernatants

HPDL cells were seeded at a density of 5×10^5 cells in 100-mm culture dishes (Corning Laboratory Sciences Company, Corning, NY, USA) and grown in standard medium. When the monolayers were confluent, the cells were rinsed twice with Hanks' balanced salt solution and incubated in 10% FCS-αMEM in the absence or presence of FGF-2 (1–50 ng/ml). At the end of the incubation periods, the supernatants were collected and stored at −20 °C until determination of HS levels. The HS levels in culture supernatants were measured by an enzyme-linked immunosorbent assay (HS assay kit, Seikagaku Co., Tokyo, Japan), following the manufacturer's instructions. Samples or HS standards were added to the wells which were coated with an anti-HS antibody, and incubated at 4 °C for 24 h. After washing, bound HS was detected by incubating with a biotinylated-antibody specific for HS and horse radish peroxidase (HRP)-conjugated streptavidin for 1 h at room temperature. The plates were washed, loaded with 3,3′,5,5′-tetramethylbenzidene substrate solution and incubated at room temperature before the reaction was stopped with stop solution. Absorbance was measured by a microplate reader (MTP-32; Corona Electric, Hitachinaka, Japan) set at 450 nm/630 nm. The HS levels in samples were calculated from the HS standard curve.

In order to determine the optimal dose of each cytokine for comparison in this study, we preliminarily examined the proliferative responses of HPDL cells induced by the cytokines. A non-saturating dose, which induced nearly equal responses among the cytokines, was selected as an optimal dose of each cytokine in this study. The doses for comparison of FGF-2, epidermal growth factor (EGF), hepatocyte growth factor (HGF), insulin like growth factor-1 (IGF-1), platelet-derived growth factor-BB (PDGF-BB), and transforming growth factor-β (TGF-β) were 50, 100, 50, 50, 50, and 10 ng/ml, respectively.

2.5. Immunocytochemical analysis

HPDL cells were seeded at a density of 5×10^3 cells in 35-mm glass bottom dishes (Matsunami Glass Ind. Ltd., Kishiwada, Japan) and cultured until confluency. At the time of the assay, culture medium was replaced with fresh medium, supplemented with 10% FCS, in the absence or presence of FGF-2 (50 ng/ml). Cells were cultured at 37 °C for the indicated times.

Cell monolayers were fixed with acetone or 2% paraformaldehyde for 10 min, then blocked with 1% bovine serum albumin (BSA) and 10% goat serum in PBS at room temperature for 30 min. The primary antibodies used were: mouse anti-human syndecan-1 antibody (Serotec Ltd., Kidlington, Oxford, UK); goat anti-human syndecan-2 antibody (Santa Cruz Biotechnology Inc., Santa Cruz, California, USA); goat anti-syndecan-4 antibody (Santa Cruz Biotechnology Inc.); mouse monoclonal biotinylated anti-hyaluronan antibody (10E4; Seikagaku Co.). Monolayers were washed three times with PBS to remove unbound antibody, then incubated for 30 min at 37 °C with Alexa Fluor 488-labeled polyclonal anti-mouse or goat IgG antibodies (Molecular Probes, Carlshad, CA, USA) or Alesa Fluor 568-labeled streptavidin (Molecular Probes). The samples were mounted on coverslipped, then viewed using an OLYMPUS 1×70 microscope (Tokyo, Japan) and photographed.

2.6. FACS analysis

HPDL cells were incubated in 10% FCS-αMEM in the absence or presence of FGF-2 (50 ng/ml). At the time of the assay, cells were incubated with mouse anti-human syndecan-1 antibody (Serotec Ltd.), goat anti-human syndecan-2 antibody (Santa Cruz Biotechnology Inc.), and biotin-conjugated mouse anti-syndecan-4 antibody (Santa Cruz Biotechnology Inc.) as primary antibodies. The cells were washed three times with PBS and incubated for 30 min at 37 °C with or without FITC-labeled polyclonal anti-mouse antibody (Caltag Laboratories, Burlingame, CA, USA),

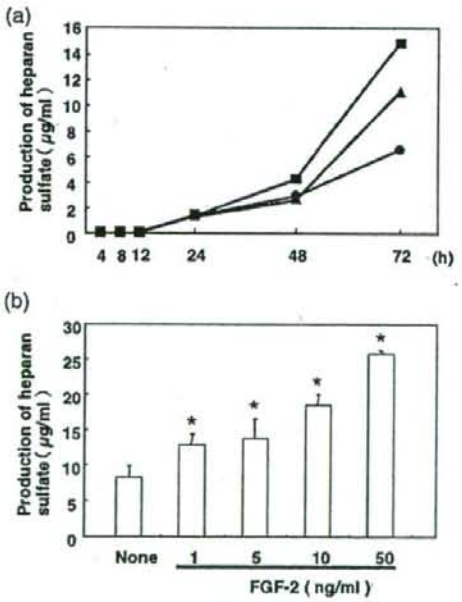

Fig. 1. Effect of FGF-2 on the production of HS by HPDL cells. HPDL cells were cultured in the absence (●) or presence of FGF-2 (5: ▲, 50: ■ ng/ml) and cultured for the indicated times (a.). HPDL cells were cultured in the absence or presence of FGF-2 (1, 5, 10, 50 ng/ml) for 72 h (b.). Conditioned medium was removed and the level of HS analyzed using an enzyme-linked immunosorbent assay. Results of one representative experiment from three separate experiments are shown. (*$p<0.05$ compared to unstimulated control).

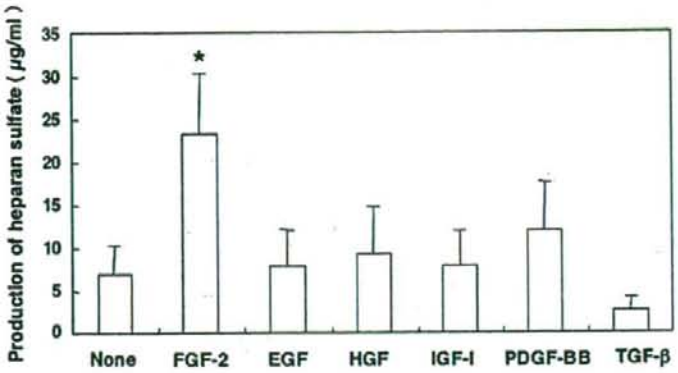

Fig. 2. Effect of various cytokines on HS production by HPDL cells. HPDL cells were cultured without any cytokine or with FGF-2 (50 ng/ml), EGF (100 ng/ml), HGF (50 ng/ml), IGF-1 (50 ng/ml), PDGF-BB (50 ng/ml), or TGF-β (10 ng/ml). Culture supernatants were removed after 72 h of exposure to the various cytokines, and the HS concentration measured by enzyme-linked immunosorbent assay. Results of one representative experiment from three separate experiments are shown. (*$p<0.05$ compared to unstimulated control).

FITC-labeled polyclonal anti-goat antibody (Santa Cruz Biotechnology Inc.), or FITC-labeled streptavidin (BD Biosciences, San Diego, CA).

2.7. Dot blot analysis

Medium from FGF-2-stimulated or unstimulated HPDL cells was collected, and a 400-μl sample spotted onto a nitrocellulose membrane. The membrane was blocked for 1 h with PBS containing 10% BSA, incubated overnight at 4 °C with a mouse monoclonal antibody to syndecan-1, -2, or -4, or a goat polyclonal antibody to glypican-1 (Santa Cruz), -2 (R&D Systems, Inc., Minneapolis, MN, USA), -3 (Santa Cruz), -6 (R&D Systems, Inc.), or perlecan (Santa Cruz), washed with PBS containing 1% BSA, and then incubated with HRP-conjugated rabbit anti-mouse serum or anti-goat serum. Immunoreactive bands were identified using a chemiluminescent kit (ECL, Amersham Pharmacia Biotech, Piscataway, NJ, USA), and were scanned densitometrically and analyzed using NIH image 1.63.

2.8. Statistical analysis

Data are expressed as mean±standard deviation, and were compared by ANOVA and *post-hoc* Scheffé's comparisons.

3. Results

3.1. FGF-2 induced production of HS by HPDL cells, but did not affect the production of HS biosynthesis-associated enzymes

Although FGF-2 has been reported to modulate extracellular matrix production, the effects of FGF-2 on glycosaminoglycan production by HPDL cells have not been fully elucidated (Shimabukuro et al., 2005). Focusing on HS production by HPDL cells, we first analyzed the concentration of HS in conditioned medium of FGF-2-stimulated HPDL cells. HS (1.29 μg/ml) was detected in the culture supernatants after 24 h of stimulation. The concentration of HS was found to gradually increase during 72 h of stimulation, with the increase

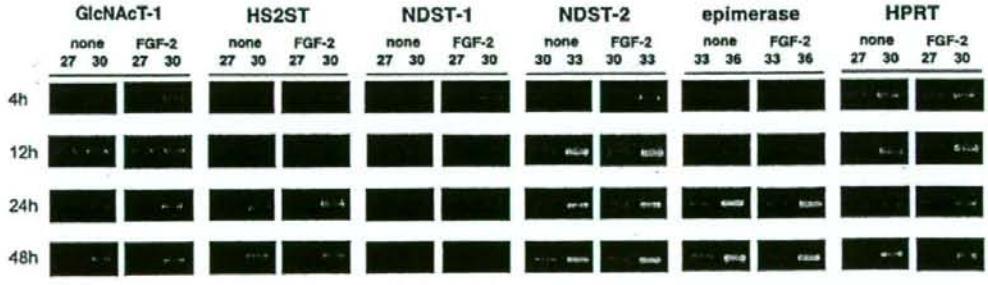

Fig. 3. mRNA expression of HS synthetic enzymes in HPDL cells. The expression of mRNA of HS-related enzymes in HPDL cells cultured in the absence or presence of FGF-2 (50 ng/ml) for 24 h was measured. Total RNA was recovered and RT-PCR performed to analyze the mRNA expression of GlcNAcT-1, HS2ST, NDST-1, NDST-2, epimerase, and HPRT in HPDL cells. Results of one representative experiment from three separate experiments are shown. The number of PCR amplification cycles is shown above each lane.

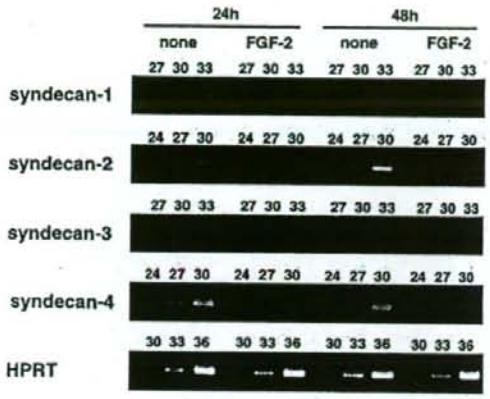

Fig. 4. mRNA expression of the syndecan gene family in HPDL cells. The expression of mRNA of the syndecan gene family in HPDL cells cultured in the absence or presence of FGF-2 (50 ng/ml) for 24 h and 48 h was measured. Total RNA was recovered and RT-PCR performed to analyze the mRNA expression of syndecan-1, -2, -3, and -4, and HPRT in HPDL cells. Results of one representative experiment from three separate experiments are shown. The number of PCR amplification cycles is shown above each lane.

between 48 and 72 h being particularly pronounced. In addition, the amount of HS produced was dependent on the dose of FGF-2 (Fig. 1).

The effects of other cytokines on the production of HS were then investigated, as production of HS can be modulated by various factors. In contrast to the marked effect of FGF-2, PDGF-BB slightly stimulated and TGF-β weakly suppressed the production of HS by HPDL cells, and the other cytokines examined (EGF, HGF, and IGF-1) did not alter HS production (Fig. 2). However, minor effects of PDGF-BB and TGF-β were not statistically significant.

HS synthesis is extended with *N*-acetyl-glucosamine (GlcNAc) from the four initial monosaccharides, and the growing glycosaminoglycan chains are modified by epimerazation, deacetylation/*N*-sulfation, and *O*-sulfation (Prydz and Dalen, 2000). Thus, we used semi-quantitative RT-PCR to examine the gene expressions of enzymes involved in the biosynthesis of HS 4, 12, 24 and 48 h after FGF-2 stimulation. However, we found that gene expressions of *N*-acetylglucosaminyltransferase (GlcNAcT)-1, heparan sulfate 2-*O*-sulfotransferase (HS2ST), *N*-deacetylase/*N*-sulfotransferase (NDST)-1, NDST-2, epimerase,

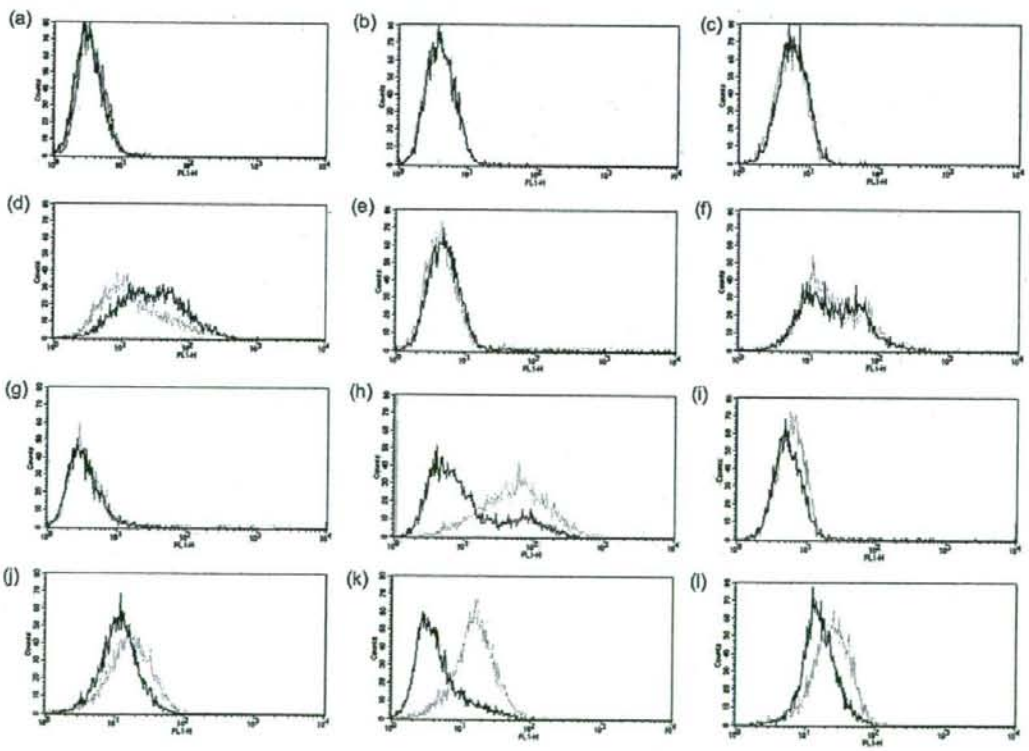

Fig. 5. FACS analysis of syndecan expression on HPDL cells. HPDL cells were incubated in 10% FCS-αMEM in the absence (gray line) or presence of FGF-2 (50 ng/ml) (black line) for 24 h (a, d, g, j), 48 h (b, e, h, k) or 72 h (c, f, i, l). At the time of the assay, cells were incubated without (a, b, c) or with the following primary antibodies: mouse anti-human syndecan-1 antibody (d, e, f); goat anti-human syndecan-2 antibody (g, h, i); mouse anti-syndecan-4 antibody (j, k, l). The cells were washed three times with PBS and incubated for 30 min at 37 °C with or without a biotinylated polyclonal anti-mouse or anti-goat antibody. After washing with PBS, staining was achieved with streptavidin-FITC.

and HPRT were not altered in FGF-2-stimulated HPDL cells at any time points examined (Fig. 3).

3.2. FGF-2 modulated syndecan expression by HPDL cells

Syndecan proteoglycan is the principal source of cell surface HS. To study the effects of FGF-2 on mRNA expression of the syndecan family in HPDL cells, RT-PCR was performed. In unstimulated HPDL cells, the mRNAs of syndecan-1 and -2 were weakly expressed and that of syndecan-4 was moderately expressed; syndecan-3 mRNA was not detected. When the HPDL cells were stimulated with FGF-2 for 24 and 48 h, the gene expression of syndecan-1, -2, and -4 was suppressed (Fig. 4).

HS proteoglycans on the cell surface are known to be shed from the cell surface into culture medium by proteolytic enzymes (Bernfield et al., 1999; Hooper et al., 1997). Next, we used FACS and immunocytochemical analyses to examine whether surface expression of HS proteoglycans on HPDL cells could be altered by FGF-2 treatment. Since syndecan-3 mRNA was not detected in either unstimulated or FGF-2-stimulated HPDL cells, we examined the expression of syndecan-1, -2, and -4 on HPDL cells. As shown in Fig. 5 FACS analysis revealed that FGF-2 lowered the expressions of syndecan-2 and -4, after 48 h and 72 h stimulation with FGF-2 and did not alter the expression of syndecan-1 on the surface of HPDL cells (Fig. 5) at any time point examined.

All three HPDL cell lines showed the decreased syndecan-2 and -4 expression in response to FGF-2 although the extent of these syndecan expression was slightly different among the cell lines. In order to confirm these alterations in HS expression on FGF-2-stimulated HPDL cells, immunocytochemical experiments were also performed. Consistent with the results of FACS experiments, expression of syndecan-2 and -4 on HPDL decreased after FGF-2 stimulation (data not shown).

Using dot blot analysis, we further examined the role of shedded syndecan in the enhanced secretion of HS in the culture supernatant of FGF-2-stimulated HPDL cells. The amounts of syndecan-1 and -2 detected in the culture supernatants of unstimulated HPDL cells were changed during the culture period. Medium from HPDL cells stimulated with FGF-2 showed no change in the amounts of syndecan-1 and -2. However, a significant increase in the amount of syndecan-4 was observed (Fig. 6). Although glypican-1, -2, -3, -6 and perlecan were also investigated, these HS proteoglycans were not detectable and no differences were observed between FGF-2-stimulated and unstimulated HPDL (data not shown).

4. Discussion

HS proteoglycan, which is composed of a core protein and HS chains, is prevalent on the cell surface and basement membrane, and has been shown to regulate various cell behaviors. It mediates signaling via interaction with matrix molecules, growth factors, or matrix metalloproteinases (MMPs). The syndecan family of four transmembrane proteoglycans is a main source of HS at cell surfaces. In this study, FGF-2 enhanced the concentration of HS in the culture medium of HPDL cells, and differentially regulated the expression of syndecan family members on the cell surface (Fig. 5). Of particular note is the fact that the level of HS in conditioned medium of FGF-2-stimulated HPDL cells was elevated in the presence of specific regulation of syndecan family members (Fig. 6). These observations suggest that individual syndecan family members may play distinct roles in response to FGF-2 (Kim et al., 1994; Lories et al., 1992).

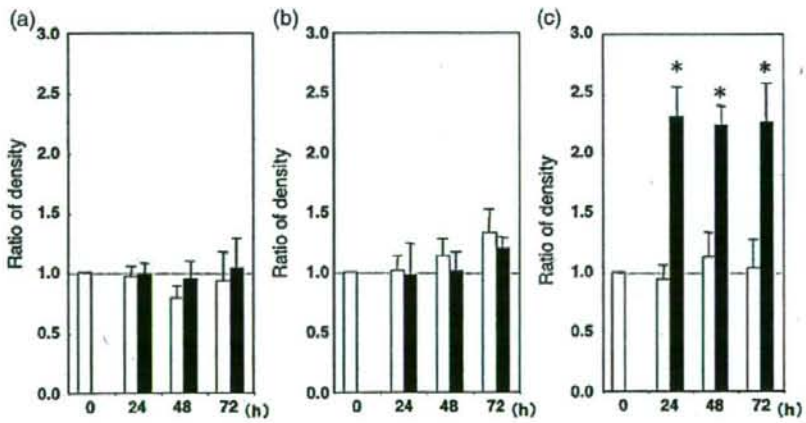

Fig. 6. Dot blot analysis of shedded syndecan in the culture supernatant of HPDL cells. Medium from FGF-2 (50 ng/ml)-stimulated (closed column) or unstimulated (open column) HPDL cells was collected after 24, 48, or 72 h. Nitrocellulose membrane was spotted with each sample, and blocked with 10% BSA to minimise non-specific binding. The membrane was incubated with HRP-conjugated rabbit anti-mouse serum for 1 h following overnight treatment with a mouse monoclonal antibody to syndecan-1 (a), -2 (b), or -4 (c). Immunoreactive bands were visualized by a chemiluminescent reaction. Data were expressed as a ratio of densitometric units relative to the value at hour 0. The experiments were performed by using these different HPDL cell lines. Mean ratios and standard deviations of the data obtained from all these cell lines are expressed in this figure ($p<0.05$ compared to unstimulated control).

HS, a highly-sulfated glycosaminoglycan, is synthesized via multiple processes during which a series of enzymes is involved in the polymerization and modification of the HS chain. The expression of these enzymes has been reported to be regulated by several factors (Clasper et al., 1999; Moreira et al., 2003). However, FGF-2 did not activate the gene expression of the HS biosynthetic enzymes examined in this study (Fig. 3). In addition, the gene expressions of syndecan (Fig. 4) and glypican (data not shown), both of which are major HS proteoglycans on the HPDL cell surface, were not increased. These results suggest that up-regulation of the biosynthesis of HS proteoglycan does not play a major role in the elevation of the level of HS in FGF-2-stimulated HPDL cell culture medium. However, the fact that no changes in the above-mentioned genes were observed may be a timing issue. Thus, the timing may be one aspects that needs further studies.

Membrane-bound proteins such as CD43, CD44, tumor necrosis factor-α receptor, IL-6 receptor, and the syndecans are cleaved by proteolytic enzymes, sheddase or secretase, and subsequently function as soluble factors (Hooper et al., 1997). The syndecans and glypican are major cell surface proteoglycans and can be shed by proteolytic cleavage of their core proteins (David et al., 1990; Kato et al., 1998). In this study, FACS analysis revealed FGF-2-induced reduction of syndecan-2 and -4 expression on the HPDL cell surface (Fig. 5). Furthermore, dot blot analysis demonstrated an increased level of syndecan-4 in conditioned medium of FGF-2-activated HPDL cells (Fig. 6). These results suggest that FGF-2 treatment results in the loss of cell surface syndecan-4, with a concomitant increase in the level of syndecan-4 in the conditioned medium. Therefore, the current findings support the hypothesis that syndecan-4 is shed from FGF-2-activated HPDL cell surfaces. However, the mechanism of the release of each syndecan from the cell surface seems to differ with the individual syndecan family member, as the expression of each syndecan was altered differently.

Shedding of syndecan is accelerated by various factors via several intracellular signaling molecules, including extracellular signal-regulated kinase and protein kinase C, and involves the proteolytic activity responsible for cleavage of syndecan ectodomain which is regulated by MMPs and tissue inhibitors of metalloproteinases (TIMPs) (Endo et al., 2003; Fitzgerald et al., 2000; Subramanian et al., 1997). In fact, it has been reported that FGF-2 modulates the activities of some MMPs and TIMPs (Liu et al., 2002; Pintucci et al., 2003; Yasui et al., 2004). Interestingly, TIMP-3 has been reported to inhibit shedding of syndecan-1 and -4 ectodomain (Fitzgerald et al., 2000), and MMP-7 has been reported to be associated with syndecan shedding (Li et al., 2002). However, exogenous addition of these molecules to the culture medium did not affect the release of HS

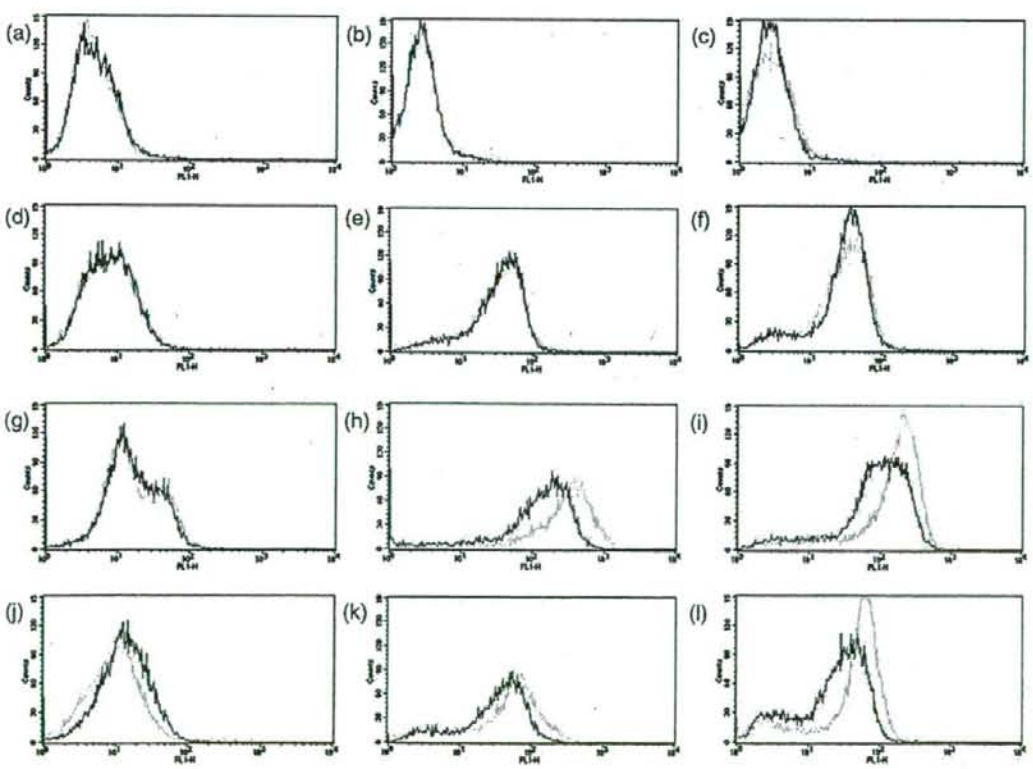

Appendix data 1.

from HPDL cells (data not shown). Further investigation is needed to clarify the mechanism by which cleavage of syndecan family members, particularly syndecan-4, occurs.

Whereas an increased level of syndecan-4 in conditioned medium of FGF-2-activated HPDL cells and a suppression of syndecan-4 expression on FGF-2-stimulated HPDL cells were observed, FGF-2 did not change the level of syndecan-2 in conditioned medium, but decreased its surface expression. HS proteoglycans on the cell surface are constitutively internalized (Yanagishita and Hascall, 1984), and FGF-2 is also internalized by both HS proteoglycan and FGF receptor (Reiland and Rapraeger, 1993; Roghani and Moscatelli, 1992). Thus, surface syndecan-2 on HPDL cells may be internalized from the cell surface following treatment of HPDL cells with FGF-2.

Glypicans are HS proteoglycans which are anchored to cell membrane via a glycosyl phosphatidyl inositol linkage. They comprise a family of six genes in mammals. Perlecan is also one of HS proteoglycan, known to be an important component of basement membrane like collagen type IV and laminin and takes part in wound healing and angiogenesis. As both HS proteoglycan are known to cleaved from cell membrane and secreted (Bernfield et al., 1999; Hacker et al., 2005), we examined their expression in the culture supernatants by dot blot analysis. However, increased expressions of glypican-1, -2, -3, -6 and perlecan were not detected in the culture supernatants of FGF-2-stimulated HPDL. Thus, it is unlikely that increase of HS in the culture supernatants of FGF-2 stimulated HPDL can be explained by shedding of those glypicans and perlecan.

It has been reported that syndecan expression was elevated at the wound edge and in lesions surrounding injured tissue, and was transiently decreased in cells migrating into the wound area (Elenius et al., 1991; Gallo et al., 1996; Iseki et al., 2002). Impaired wound healing and angiogenesis in mice lacking syndecan-4 (Echtermeyer et al., 2001), and delayed migration of corneal epithelial cells in mice lacking syndecan-1 (Stepp et al., 2002) have been observed. Over-expression of syndecan-1 and prolonged shedding is associated with delayed wound healing (Elenius et al., 2004), and reduced proliferation rate at the wound edge was also noted. Moreover, a recent study showed that cleavage of syndecan-1 was involved in cell migration (Endo et al., 2003). Also, it has been demonstrated that soluble syndecan ectodomain promotes cell growth (Yang et al., 2002), and that syndecan ectodomains accumulate in wound fluid (Subramanian et al., 1997). These findings suggest that,

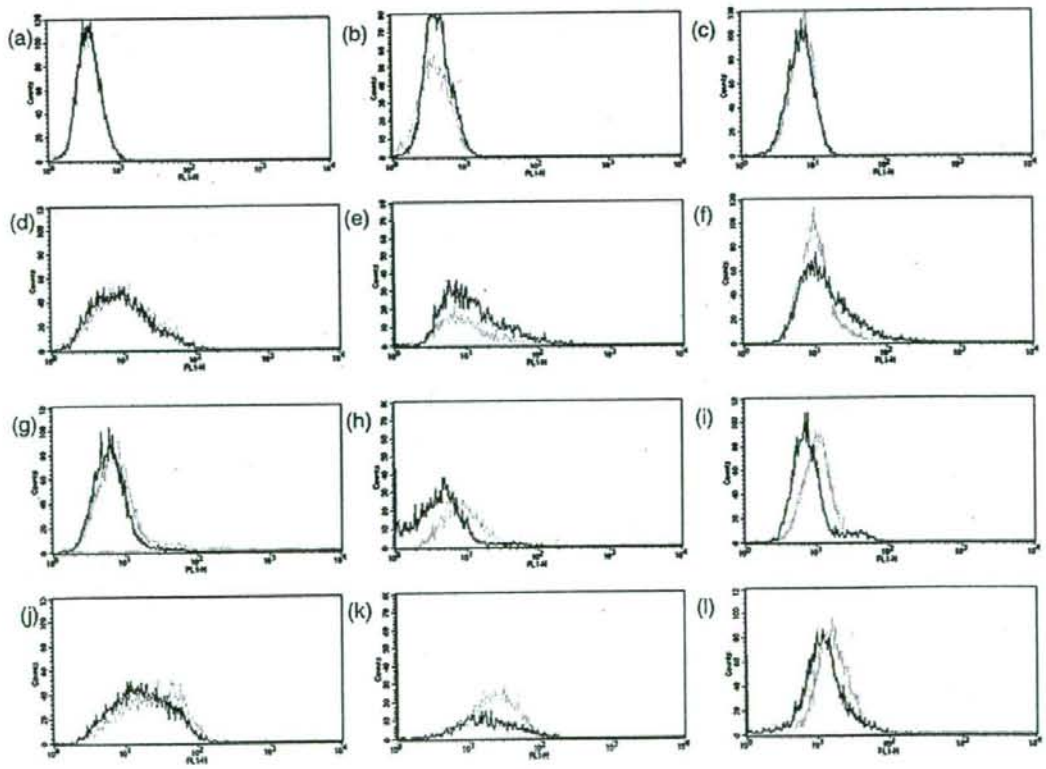

Appendix data 2.

not only the cell surface, but also the shed syndecans are closely associated with wound healing. Therefore, it is possible that FGF-2-induced shedding and accumulation of HS proteoglycan are associated with the effects of FGF-2 on acceleration of wound healing and subsequent tissue regeneration.

A close relationship between the actions of HS and FGF has also been reported (Rapraeger et al., 1991; Yayon et al., 1991). Shed proteoglycan can bind HS-binding proteins such as FGF-2 and modulate the functional effects via regulation of binding activity to receptors (Kato et al., 1998). Whether exogenous HS proteoglycans prevent or activate FGF-2 binding to FGF receptors (Bernfield et al., 1999; Kato et al., 1998; Mali et al., 1993; Modrowski et al., 2000) is dependent on the source and composition of the HS proteoglycan. Although the detailed mechanism by which shed HS or HS proteoglycan regulate FGF-2 activity remains elusive, released HS appears to modulate the interaction between FGF-2 and its receptor.

FGF-2 has been recognized to play a critical role in tissue regeneration. Indeed, it is detected at the wound (Crowley et al., 1995; Flaumenhaft et al., 1992; Murakami et al., 1999). It is postulated that in injured tissue, release of FGF-2, which is trapped to HS at the cell surface, is enhanced through proteolytic enzymes (Flaumenhaft et al., 1989). In addition, HS itself is a major constituent of tissue matrices and appears to play modulatory roles in tissue remodeling. Furthermore, we have previously reported that FGF-2 prompted regeneration of periodontal tissue that had been destroyed by the progression of periodontal diseases (Murakami et al., 1999, 2003; Takayama et al., 2001). The present observation that FGF-2 increases the level of HS in the HPDL cell culture supernatant suggests positive or negative feedback regulation during wound healing and regeneration processes in damaged periodontal tissues.

Acknowledgements

This work was supported by Grants-in-Aid for Scientific Research (the Japan Society for the Promotion of Science Nos. 17390560, 17209065 and 17390561, 18659622, 18791591, 18890107) and the 21st Century COE entitled, "Origination of Frontier BioDentistry", Osaka University Graduate School of Dentistry supported by the Ministry of Education, Culture, Sports, Science and Technology. We thank Kaken Pharmaceutical Co. Ltd. and Seikagaku Co. for providing technical assistance, valuable reagents and advice.

Appendix A

Appendix data 1 and 2 FACS analysis of syndecan expression on HPDL cells. HPDL cells (the other cells than that in Fig. 5) were incubated in 10% FCS-αMEM in the absence (gray line) or presence of FGF-2 (50 ng/ml) (black line) for 24 h (a, d, g, j), 48 h (b, e, h, k) or 72 h (c, f, i, l). At the time of the assay, cells were incubated without (a, b, c) or with the following primary antibodies: mouse anti-human syndecan-1 antibody (d, e, f); goat anti-human syndecan-2 antibody (g, h, i); mouse anti-syndecan-4 antibody (j, k, l). The cells were washed three times with PBS and incubated for 30 min at 37 °C with or without a biotinylated polyclonal anti-mouse or anti-goat antibody. After washing with PBS, staining was achieved with streptavidin-FITC.

References

Bernfield, M., Gotte, M., Park, P.W., Reizes, O., Fitzgerald, M.L., Lincecum, J., Zako, M., 1999. Functions of cell surface heparan sulfate proteoglycans. Annu. Rev. Biochem. Allied Res. India 68, 729–777.

Bikfalvi, A., Klein, S., Pintucci, G., Rifkin, D.B., 1997. Biological roles of fibroblast growth factor-2. Endocr. Rev. 18, 26–45.

Clasper, S., Vekemans, S., Fiore, M., Plebanski, M., Wordsworth, P., David, G., Jackson, D.G., 1999. Inducible expression of the cell surface heparan sulfate proteoglycan syndecan-2 (fibroglycan) on human activated macrophages can regulate fibroblast growth factor action. J. Biol. Chem. 274, 24113–24123.

Crowley, S.T., Ray, C.J., Nawaz, D., Majack, R.A., Horwitz, L.D., 1995. Multiple growth factors are released from mechanically injured vascular smooth muscle cells. Am. J. Physiol. 269, H1641–H1647.

David, G., Lories, V., Decock, B., Marynen, P., Cassiman, J.J., Van den Berghe, H., 1990. Molecular cloning of a phosphatidylinositol-anchored membrane heparan sulfate proteoglycan from human lung fibroblasts. J. Cell Biol. 111, 3165–3176.

Echtermeyer, F., Streit, M., Wilcox-Adelman, S., Saoncella, S., Denhez, F., Detmar, M., Goetinck, P., 2001. Delayed wound repair and impaired angiogenesis in mice lacking syndecan-4. J. Clin. Invest. 107, R9–R14.

Elenius, K., Vainio, S., Laato, M., Salmivirta, M., Thesleff, I., Jalkanen, M., 1991. Induced expression of syndecan in healing wounds. J. Cell Biol. 114, 585–595.

Elenius, K., Paul, S., Allison, G., Sun, J., Klagsbrun, M., 1997. Activation of HER4 by heparin-binding EGF-like growth factor stimulates chemotaxis but not proliferation. EMBO J. 16, 1268–1278.

Elenius, V., Gotte, M., Reizes, O., Elenius, K., Bernfield, M., 2004. Inhibition by the soluble syndecan-1 ectodomains delays wound repair in mice overexpressing syndecan-1. J. Biol. Chem. 279, 41928–41935.

Endo, K., Takino, T., Miyamori, H., Kinsen, H., Yoshizaki, T., Furukawa, M., Sato, H., 2003. Cleavage of syndecan-1 by membrane type matrix metalloproteinase-1 stimulates cell migration. J. Biol. Chem. 278, 40764–40770.

Fitzgerald, M.L., Wang, Z., Park, P.W., Murphy, G., Bernfield, M., 2000. Shedding of syndecan-1 and -4 ectodomains is regulated by multiple signaling pathways and mediated by a TIMP-3-sensitive metalloproteinase. J. Cell Biol. 148, 811–824.

Flaumenhaft, R., Moscatelli, D., Saksela, O., Rifkin, D.B., 1989. Role of extracellular matrix in the action of basic fibroblast growth factor: matrix as a source of growth factor for long-term stimulation of plasminogen activator production and DNA synthesis. J. Cell. Physiol. 140, 75–81.

Flaumenhaft, R., Abe, M., Mignatti, P., Rifkin, D.B., 1992. Basic fibroblast growth factor-induced activation of latent transforming growth factor beta in endothelial cells: regulation of plasminogen activator activity. J. Cell Biol. 118, 901–909.

Gallo, R., Kim, C., Kokenyesi, R., Adzick, N.S., Bernfield, M., 1996. Syndecans-1 and -4 are induced during wound repair of neonatal but not fetal skin. J. Invest. Dermatol. 107, 676–683.

Hacker, U., Nybakken, K., Perrimon, N., 2005. Heparan sulphate proteoglycans: the sweet side of development. Nat. Rev., Mol. Cell Biol. 6, 530–541.

Hooper, N.M., Karran, E.H., Turner, A.J., 1997. Membrane protein secretases. Biochem. J. 321, 265–279.

Iseki, K., Hagino, S., Mori, T., Zhang, Y., Yokoya, S., Takaki, H., Tase, C., Murakawa, M., Wanaka, A., 2002. Increased syndecan expression by pleiotrophin and FGF receptor-expressing astrocytes in injured brain tissue. Glia 39, 1–9.

Ishiguro, K., Kadomatsu, K., Kojima, T., Muramatsu, H., Nakamura, E., Ito, M., Nagasaka, T., Kobayashi, H., Kusugami, K., Saito, H., Muramatsu, T., 2000. Syndecan-4 deficiency impairs the fetal vessels in the placental labyrinth. Dev. Dyn. 219, 539–544.

Kainulainen, V., Wang, H., Schick, C., Bernfield, M., 1998. Syndecans, heparan sulfate proteoglycans, maintain the proteolytic balance of acute wound fluids. J. Biol. Chem. 273, 11563–11569.

Kato, M., Wang, H., Kainulainen, V., Fitzgerald, M.L., Ledbetter, S., Ornitz, D.M., Bernfield, M., 1998. Physiological degradation converts the soluble syndecan-

1 ectodomain from an inhibitor to a potent activator of FGF-2. Nat. Med. 4, 691–697.

Kim, C.W., Goldberger, O.A., Gallo, R.L., Bernfield, M., 1994. Members of the syndecan family of heparan sulfate proteoglycans are expressed in distinct cell-, tissue-, and development-specific patterns. Mol. Biol. Cell 5, 797–805.

Li, Q., Park, P.W., Wilson, C.L., Parks, W.C., 2002. Matrilysin shedding of syndecan-1 regulates chemokine mobilization and transepithelial efflux of neutrophils in acute lung injury. Cell 111, 635–646.

Liu, J.F., Crepin, M., Liu, J.M., Barritault, D., Ledoux, D., 2002. FGF-2 and TPA induce matrix metalloproteinase-9 secretion in MCF-7 cells through PKC activation of the Ras/ERK pathway. Biochem. Biophys. Res. Commun. 293, 1174–1182.

Lories, V., Cassiman, J.J., Van den Berghe, H., David, G., 1992. Differential expression of cell surface heparan sulfate proteoglycans in human mammary epithelial cells and lung fibroblasts. J. Biol. Chem. 267, 1116–1122.

Mali, M., Elenius, K., Miettinen, H.M., Jalkanen, M., 1993. Inhibition of basic fibroblast growth factor-induced growth promotion by overexpression of syndecan-1. J. Biol. Chem. 268, 24215–24222.

Modrowski, D., Basle, M., Lomri, A., Marie, P.J., 2000. Syndecan-2 is involved in the mitogenic activity and signaling of granulocyte-macrophage colony-stimulating factor in osteoblasts. J. Biol. Chem. 275, 9178–9185.

Moreira, C.R., Porcionatto, M.A., Dietrich, C.P., Nader, H.B., 2003. Effect of bradykinin and PMA on the synthesis of proteoglycans during the cell cycle of endothelial cells in culture. Int. J. Immunopharmacol. 3, 293–298.

Murakami, S., Takayama, S., Ikezawa, K., Shimabukuro, Y., Kitamura, M., Nozaki, T., Terashima, A., Asano, T., Okada, H., 1999. Regeneration of periodontal tissues by basic fibroblast growth factor. J. Periodontal Res. 34, 425–430.

Murakami, S., Takayama, S., Kitamura, M., Shimabukuro, Y., Yanagi, K., Ikezawa, K., Saho, T., Nozaki, T., Okada, H., 2003. Recombinant human basic fibroblast growth factor (bFGF) stimulates periodontal regeneration in class II furcation defects created in beagle dogs. J. Periodontal Res. 38, 97–103.

Nugent, M.A., Iozzo, R.V., 2000. Fibroblast growth factor-2. Int. J. Biochem. Cell Biol. 32, 115–120.

Park, P.W., Pier, G.B., Preston, M.J., Goldberger, O., Fitzgerald, M.L., Bernfield, M., 2000. Syndecan-1 shedding is enhanced by LasA, a secreted virulence factor of *Pseudomonas aeruginosa*. J. Biol. Chem. 275, 3057–3064.

Pintucci, G., Yu, P.J., Sharony, R., Baumann, F.G., Saponara, F., Frasca, A., Galloway, A.C., Moscatelli, D., Mignatti, P., 2003. Induction of stromelysin-1 (MMP-3) by fibroblast growth factor-2 (FGF-2) in FGF-2−/− microvascular endothelial cells requires prolonged activation of extracellular signal-regulated kinases-1 and -2 (ERK-1/2). J. Cell. Biochem. 90, 1015–1025.

Prydz, K., Dalen, K.T., 2000. Synthesis and sorting of proteoglycans. J. Cell Sci. 113, 193–205.

Rapraeger, A.C., Krufka, A., Olwin, B.B., 1991. Requirement of heparan sulfate for bFGF-mediated fibroblast growth and myoblast differentiation. Science 252, 1705–1708.

Reiland, J., Rapraeger, A.C., 1993. Heparan sulfate proteoglycan and FGF receptor target basic FGF to different intracellular destinations. J. Cell Sci. 105, 1085–1093.

Roghani, M., Moscatelli, D., 1992. Basic fibroblast growth factor is internalized through both receptor-mediated and heparan sulfate-mediated mechanisms. J. Biol. Chem. 267, 22156–22162.

Shimabukuro, Y., Ichikawa, T., Takayama, S., Yamada, S., Takedachi, M., Terakura, M., Hashikawa, T., Murakami, S., 2005. Fibroblast growth factor-2 regulates the synthesis of hyaluronan by human periodontal ligament cells. J. Cell. Physiol. 203, 557–563.

Somerman, M.J., Archer, S.Y., Imm, G.R., Foster, R.A., 1988. A comparative study of human periodontal ligament cells and gingival fibroblasts in vitro. J. Dent. Res. 67, 66–70.

Stepp, M.A., Gibson, H.E., Gala, P.H., Iglesia, D.D., Pajoohesh-Ganji, A., Pal-Ghosh, S., Brown, M., Aquino, C., Schwartz, A.M., Goldberger, O., Hinkes, M.T., Bernfield, M., 2002. Defects in keratinocyte activation during wound healing in the syndecan-1-deficient mouse. J. Cell Sci. 115, 4517–4531.

Subramanian, S.V., Fitzgerald, M.L., Bernfield, M., 1997. Regulated shedding of syndecan-1 and -4 ectodomains by thrombin and growth factor receptor activation. J. Biol. Chem. 272, 14713–14720.

Takayama, S., Murakami, S., Shimabukuro, Y., Kitamura, M., Okada, H., 2001. Periodontal regeneration by FGF-2 (bFGF) in primate models. J. Dent. Res. 80, 2075–2079.

Yanagishita, M., Hascall, V.C., 1984. Metabolism of proteoglycans in rat ovarian granulosa cell culture. Multiple intracellular degradative pathways and the effect of chloroquine. J. Biol. Chem. 259, 10270–10283.

Yang, Y., Yaccoby, S., Liu, W., Langford, J.K., Pumphrey, C.Y., Theus, A., Epstein, J., Sanderson, R.D., 2002. Soluble syndecan-1 promotes growth of myeloma tumors in vivo. Blood 100, 610–617.

Yasui, H., Andoh, A., Bamba, S., Inatomi, O., Ishida, H., Fujiyama, Y., 2004. Role of fibroblast growth factor-2 in the expression of matrix metalloproteinases and tissue inhibitors of metalloproteinases in human intestinal myofibroblasts. Digestion 69, 34–44.

Yayon, A., Klagsbrun, M., Esko, J.D., Leder, P., Ornitz, D.M., 1991. Cell surface, heparin-like molecules are required for binding of basic fibroblast growth factor to its high affinity receptor. Cell 64, 841–848.

MOLECULAR AND CELLULAR BIOLOGY, Apr. 2008, p. 2125–2137
0270-7306/08/$08.00+0 doi:10.1128/MCB.00740-07

Vol. 28, No. 7

Inducible Expression of Chimeric EWS/ETS Proteins Confers Ewing's Family Tumor-Like Phenotypes to Human Mesenchymal Progenitor Cells▽†

Yoshitaka Miyagawa,[1] Hajime Okita,[1]* Hideki Nakaijima,[1] Yasuomi Horiuchi,[1] Ban Sato,[1] Tomoko Taguchi,[1] Masashi Toyoda,[3] Yohko U. Katagiri,[1] Junichiro Fujimoto,[2] Jun-ichi Hata,[1] Akihiro Umezawa,[3] and Nobutaka Kiyokawa[1]

Department of Developmental Biology, National Research Institute for Child Health and Development, 2-10-1, Okura, Setagaya-ku, Tokyo 157-8535, Japan[1]; National Research Institute for Child Health and Development, 2-10-1, Okura, Setagaya-ku, Tokyo 157-8535, Japan[2]; and Department of Reproductive Biology, National Research Institute for Child Health and Development, 2-10-1, Okura, Setagaya-ku, Tokyo 157-8535, Japan[3]

Received 27 April 2007/Returned for modification 13 July 2007/Accepted 7 January 2008

Ewing's family tumor (EFT) is a rare pediatric tumor of unclear origin that occurs in bone and soft tissue. Specific chromosomal translocations found in EFT cause EWS to fuse to a subset of ets transcription factor genes (ETS), generating chimeric EWS/ETS proteins. These proteins are believed to play a crucial role in the onset and progression of EFT. However, the mechanisms responsible for the EWS/ETS-mediated onset remain unclear. Here we report the establishment of a tetracycline-controlled EWS/ETS-inducible system in human bone marrow-derived mesenchymal progenitor cells (MPCs). Ectopic expression of both EWS/FLI1 and EWS/ERG proteins resulted in a dramatic change of morphology, i.e., from a mesenchymal spindle shape to a small round-to-polygonal cell, one of the characteristics of EFT. EWS/ETS also induced immunophenotypic changes in MPCs, including the disappearance of the mesenchyme-positive markers CD10 and CD13 and the up-regulation of the EFT-positive markers CD54, CD99, CD117, and CD271. Furthermore, a prominent shift from the gene expression profile of MPCs to that of EFT was observed in the presence of EWS/ETS. Together with the observation that EWS/ETS enhances the ability of cells to invade Matrigel, these results suggest that EWS/ETS proteins contribute to alterations of cellular features and confer an EFT-like phenotype to human MPCs.

Ewing's family tumor (EFT) is a rare childhood cancer arising mainly in bone and soft tissue. Since EFT has a poor prognosis, it is important to elucidate the underlying pathogenic mechanisms for establishing a more effective therapeutic strategy. EFT is characterized by the presence of chimeric genes composed of EWS and ets transcription factor genes (ETS) formed by specific chromosomal translocations, i.e., EWS/FLI1, t(11;22)(q24;q12); EWS/ERG, t(21;22)(q12;q12); EWS/ETV1, t(7;22)(p22;q12); EWS/E1AF, t(17;22)(q12;q12); and EWS/FEV, t(2;22)(q33;q12) (26). The products of these chimeric genes behave as aberrant transcriptional regulators and are believed to play a crucial role in the onset and progression of EFT (3, 36). Indeed, recent studies have revealed that the induction of EWS/FLI1 proteins can trigger transformation in certain cell types, including NIH 3T3 cells (36), C2C12 myoblasts (12), and murine primary bone marrow-derived mesenchymal progenitor cells (MPCs) (6, 45, 52). However, studies have also indicated that overexpression of EWS/FLI1 provokes apoptosis and growth arrest in mouse normal embryonic fibroblasts and primary human fibroblasts (10, 31), hence hampering understanding of the precise role of EWS/ETS proteins in the development of EFT. The function of EWS/ETS proteins would be greatly influenced by cell type, and thus the cells that can originate EFTs might be more susceptible to the tumorigenic effects of EWS/ETS.

Although the cell origin of EFT is still unknown, the expression of neuronal markers in spite of the occurrence in bone and soft tissues has kept open the debate as to a potential mesenchymal or neuroectodermal origin. As described above, ectopic expression of EWS/FLI1 results in dramatic changes in morphology and the formation of EFT-like tumors in murine primary bone marrow-derived MPCs but not in murine embryonic stem cells (6, 45, 52), supporting the notion that MPCs are a plausible cell origin of EFT (45). However, others argue that MPCs cannot be considered progenitors of EFT without further evidence of similarity between human EFT and MPC-EWS/FLI1-induced tumors in mice (29, 46).

The development of experimental systems using murine species is useful for elucidating the mechanisms behind the pathogenesis of EFT. However, several differences between human and murine systems cannot be ignored; these differences include the expression patterns of surface antigens in MPCs, for instance (7, 44, 51, 53). Moreover, human cells are difficult to transform in vitro, and the transformed cells of mice seem to produce a more aggressive tumor than those of hu-

* Corresponding author. Mailing address: Department of Developmental Biology, National Research Institute for Child Health and Development, 2-10-1, Okura, Setagaya-ku, Tokyo 157-8535, Japan. Phone: 81-3-3416-0181. Fax: 81-3-3417-2496. E-mail: okita@nch.go.jp.

† Supplemental material for this article may be found at http://mcb.asm.org/.

▽ Published ahead of print on 22 January 2008.

TABLE 1. Cell lines used in this study and fusion transcript types

Cell line	Diagnosis	Fusion transcript type	Reference
EES-1	EFT	EWS/FLI1 type I	20
SCCH196	EFT	EWS/FLI1 type I	21
RD-ES	EFT	EWS/FLI1 type II	5
SK-ES1	EFT	EWS/FLI1 type II	5
NCR-EW2	EFT	EWS/FLI1 type II	19
NCR-EW3	EFT	EWS/E1AF	19
W-ES	EFT	EWS/ERG	13
NB69	NB		15
NB9	NB		15
GOTO	NB		47
NRS-1	RMS	PAX3/FKHR	40

mans (1). The findings suggest the existence of undefined cell-autonomous mechanisms that render human cells resistant to malignant transformation. Therefore, the use of human cell models is ideal for clarifying how EFT develops. Models of the onset of EFT have been generated using primary fibroblasts (31) and rhabdomyosarcoma cells (23). However, these cell types are not appropriate for studying the origins of EFT, and a model that precisely recapitulates EWS/ETS-mediated EFT formation is required.

UET-13 cells are obtained by prolonging the life span of human bone marrow stromal cells by use of the retroviral transgenes hTERT and E7 (38, 50), retain the ability to differentiate into not only mesodermal derivatives but also neuronal progenitor-like cells, and are considered a good model for studying the cellular events in human MPCs. Therefore, we have examined the biological effect of EWS/ETS in human MPCs by use of UET-13 cells by exploiting tetracycline-inducible systems for expressing EWS/ETS (EWS/FLI1 and EWS/ERG). Here we report that overexpression of EWS/ETS mediates an EFT-like phenotype, including morphology, immunophenotype, and gene expression profile, with enhancement of the Matrigel invasion ability of UET-13 cells.

MATERIALS AND METHODS

Cell cultures and establishment of UET-13TR-EWS/ETS cell lines. UET-13 cells were cultured in Dulbecco's modified Eagle's medium (DMEM) with 10% Tet system approved fetal bovine serum (T-FBS) (Takara) at 37°C under a humidified 5% CO_2 atmosphere. EFT cell lines (EES-1 [20], SCCH196 [21], RD-ES and SK-ES1 [5], NCR-EW2 and NCR-EW3 [19], and W-ES [13]) and neuroblastoma (NB) cell lines (NB69 and NB9 [15] and GOTO [47]) were cultured in RPMI 1640 with 10% FBS. A rhabdomyosarcoma cell line, NRS-1 (40), was cultured in Eagle's minimal essential medium with 10% FBS. The cell lines used in this study are listed in Table 1.

UET-13 cells were seeded at a density of 5×10^4 cells per well in 24-well tissue culture plates 1 day prior to transfection. For introducing the tetracycline-inducible system, UET-13 cells were transfected with pcDNA6-TR (Invitrogen) by use of Lipofectamine 2000 (Invitrogen). After 72 h, the medium was replaced with fresh medium containing 200 μg/ml of blasticidin S (Invitrogen). Individual resistant clones were selected for a month and designated UET-13TR cells. UET-13TR cells were further transfected with pcDNA4-EWS/ETSs constructed as described below, and individual resistant clones were selected in DMEM containing 10% T-FBS and 200 to 300 μg/ml of Zeocin (Invitrogen). The Zeocin-resistant clones were expanded and tested for the induction of EWS/ETS expression upon the addition of tetracycline by use of reverse transcription-PCR (RT-PCR) as described below.

Plasmid construction. A gateway cassette (bases 1 to 1705) was amplified from pBLOCK-iT3-DEST (Invitrogen) by PCR, and the PCR product was inserted into the EcoRV site of pcDNA4-TO (Invitrogen) (termed pcDNA4-DEST). Since the type II EWS/FLI1 is a stronger transactivator than the type I product (32), we used the type II variant in the present study. EWS/ERG was isolated from W-ES, an EFT cell line, joining EWS exon 7 and ERG exon 9. Full-length EWS/FLI1 type II and EWS/ERG cDNAs were amplified from cDNAs prepared from NCR-EW2 and W-ES cells, respectively, by PCR as described below and cloned into the XmnI-EcoRV sites of pENTR11 (Invitrogen). The resulting pENTR11-EWS/ETSs were recombined with pcDNA4-DEST by use of LR recombination reaction as instructed by the manufacturer (Invitrogen) to construct the tetracycline-inducible EWS/ETS expression vector pcDNA4-EWS/ETSs.

Western blot analysis. UET-13 transfectants were cultivated with or without 3 μg/ml of tetracycline for 72 h. Western blot analysis was performed as previously described (37). Briefly, the cell lysates were prepared and separated on a 10% sodium dodecyl sulfate-polyacrylamide gel electrophoresis gel and transferred onto a polyvinylidene difluoride membrane. The membranes were blocked with 5% skimmed milk in phosphate-buffered saline (PBS) containing 0.01% Tween 20 (Sigma) and incubated with primary antibodies. As the primary antibodies, anti-Fli-1, anti-Erg-1/2/3 (Santa Cruz Biotechnology), and anti-actin (Sigma) were used. Horseradish peroxidase-conjugated anti-rabbit or anti-mouse immunoglobulin G (IgG) antibodies (DakoCytomation) were used as secondary antibodies. Blots were detected by chemiluminescence using an ECL Plus Western blotting detection system (GE Healthcare Bio-Science Corp.) and exposed to X-ray film (Kodak) for 5 to 30 min.

MTT assay and detection of apoptosis. Growth curves of UET-13 transfectants were determined using the 3-(4,5-dimethylthiazol-2-yl)-2,5-diphenyltetrazolium bromide (MTT) assay as described previously (18). The apoptosis was detected using an annexin V-fluorescein isothiocyanate (FITC) apoptosis detection kit (Biovision) according to the manufacturer's instructions and analyzed by flow cytometry (Cytomics FC500; Beckman Coulter).

Immunofluorescence analysis. After 1 week of culture in the absence or presence of tetracycline, UET-13 cells and the transfectants were harvested with 0.25% trypsin plus EDTA (IBL). The cells (2×10^5) were incubated with mouse monoclonal antibodies for 20 min. In the case of fluorescence-labeled antibodies, the cells were washed with PBS and then analyzed. In the case of primary unconjugated mouse antibodies, the cells were washed and then incubated with FITC-conjugated goat anti-mouse IgG antibody (Jackson ImmunoResearch Laboratories) for 20 min. Cell fluorescence was detected using a Cytomics FC500 instrument as described previously (27).

Antibodies against the following human antigens were used: CD10, CD13, CD14, CD29, CD34, CD40, CD44, CD45, CD49e, CD54, CD56, CD61, CD90, CD105, CD117, and CD166 from Beckman Coulter; CD73 from BD Biosciences-Pharmingen; CD55 from Abcam; CD59 from Cedarlane Laboratories; and CD133 and CD271 from Miltenyi Biotec GmbH.

Immunocytochemistry. Cells were grown on collagen type I-coated cover glasses (Iwaki). After 72 h with or without tetracycline, cells were fixed for 30 min in 4% paraformaldehyde and permeabilized in PBS containing 0.2% Triton X-100 (Sigma) for 30 min. Subsequently, they were washed with PBS and blocked in PBS containing 0.1% Triton X-100 and 1% bovine serum albumin (Sigma) for 30 min before being incubated with a monoclonal anti-CD99 antibody, i.e., 12E7 (1:100) (DakoCytomation) or O13 (1:200) (Thermo), and polyclonal anti-Fli-1 antibody (1:100) (Santa Cruz) for 1 h. Bound antibodies were visualized with appropriate secondary antibodies, i.e., Alexa Fluor 488 goat anti-mouse IgG (heavy plus light chains) highly cross-adsorbed and Alexa Fluor 546 goat anti-rabbit IgG (heavy plus light chains) highly cross-adsorbed (Invitrogen) for 1 h at 1:300. Nuclei were counterstained with 4',6'-diamidino-2-phenylindole (DAPI) or propidium iodide (PI) (Sigma). For the visualization of whole cells, cells were treated with Celltracker Blue (Invitrogen) for 30 min and then fixed. Fluorescence was observed and analyzed using a confocal laser scanning microscope and image software (either FV500 from Olympus or LSM510 from Carl Zeiss). Precise measurements of cell size, nuclear size, and the nucleus-to-cytoplasm (N/C) ratio were performed using Image J (16).

RT-PCR analysis. Total RNA was extracted from cells by use of an RNeasy kit (Qiagen) and reverse transcribed using a first-strand cDNA synthesis kit (GE Healthcare Bio-Science Corp). RT-PCR was performed with a HotstarTaq master mix kit (Qiagen). As an internal control, human GAPDH cDNA was also amplified. The sequences of gene-specific primers for RT-PCR were as follows: for EWS/FLI1 (forward), 5'-ATGGCGTCCACGGATTACAGTACCT-3'; for EWS/FLI1 (reverse), 5'-GGGTCTTCTTTGACACTCAATCG-3'; for EWS/ERG (forward), 5'-ATGGCGTCCACGGATTACAGTACCT-3'; for EWS/ERG (reverse), 5'-TTAGTAGTAAGTGCCCAGATGAGAA-3'; for GAPDH (forward), 5'-CCACCCATGGCAAATTCCATGGCA-3'; and for GAPDH (reverse), 5'-TCTAGACGGCAGGTCAGGT/CCACC-3'. PCR products were electrophoresed with a 1% agarose gel and stained with ethidium bromide.

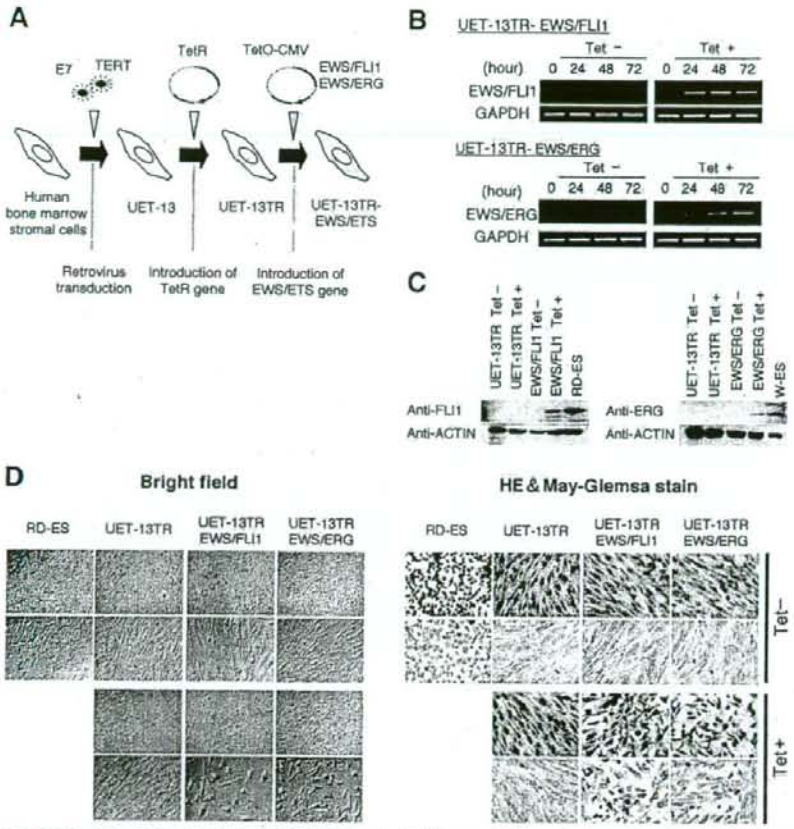

FIG. 1. The effect of EWS/ETS on the morphology of UET-13 cells. (A) The establishment of a tetracycline-inducible EWS/ETS expression system in UET-13 cells. CMV, cytomegalovirus. (B) Analyses for confirming the inducible expression of EWS/ETS genes. EWS/ETS mRNAs were detected in UET-13 transfectants UET-13TR-EWS/FLI1 and UET-13TR-EWS/ERG by RT-PCR. These cells were treated with or without 3 μg/ml of tetracycline (Tet) for the indicated periods. As an internal control, a human GAPDH gene was used. (C) Analyses for confirming the inducible expression of EWS/ETS proteins. The cells were treated as described for panel B and subjected to Western blotting for the detection of EWS/ETS proteins. The extracts of RD-ES and W-ES cells were also examined as positive controls. Membranes were reprobed with anti-actin antibody as a loading control. (D) Morphological change after tetracycline treatment of UET-13 transfectants. UET-13 cells and the transfectants were cultured in the absence or presence of tetracycline for 72 h and observed by light microscopy. Magnification, ×40 (top); ×200 (bottom). Cells were also examined using hematoxylin-eosin (HE) (top) and May-Giemsa (bottom) staining (magnification, ×200).

Real-time RT-PCR. Real-time RT-PCR was performed using TaqMan universal PCR master mix and TaqMan gene expression assays and an inventoried assay on an ABI Prism 7900HT sequence detection system (Applied Biosystems) according to the manufacturer's instructions. The human GAPDH gene was used as an internal control for normalization.

DNA microarray analysis. Total RNA isolated from cells was reverse transcribed and labeled using one-cycle target labeling and control reagents as instructed by the manufacturer (Affymetrix). The labeled probes were hybridized to the human genome U133 Plus 2.0 array (Affymetrix). The arrays were performed in a single experiment and analyzed using GeneChip operating software, version 1.2 (Affymetrix). Background subtraction, normalization, and principal component analysis (PCA) were performed by GeneSpring GX 7.3 software (Agilent Technologies). Signal intensities were prenormalized based on the median of all measurements on that chip. To account for the difference in detection efficiencies between the spots, prenormalized signal intensities on each gene were normalized to the median of prenormalized measurements for that gene. The data were filtered using the following steps. (i) Genes that were scored as absent in all samples were eliminated. (ii) Genes for which the signal intensities were lower than 100 were eliminated. (iii) Performing cluster analysis using filtering genes, we selected the genes that exhibited increased expression or decreased expression in tetracycline-treated cells. Accession numbers for the microarray data are given below.

Invasion assay. The invasion assay was performed using Matrigel (BD Bioscience) according to the previous description (34) with some modification. Polycarbonate filter inserts containing 8-μm pores (BD Falcon) were coated with 50 μl of a 6:1 mixture of culture medium and Matrigel and placed into 24-well culture plates containing DMEM supplemented with 10% T-FBS as chemoattractants. Cells (2.5×10^4) treated with or without tetracycline for 72 h were suspended in DMEM containing 0.01% T-FBS and plated on top of each filter insert. After 20 h in culture in the presence or absence of tetracycline, noninvading cells were removed from upper surface of the filter with a cotton swab. The invading cells on the lower surface of the filter were fixed with formalin, stained with hematoxylin-eosin, and counted in five fields per membrane with light microscopy. As a control, cells were also cultured on uncoated filter inserts. The invasion efficiency was presented as the ratio of the number of invading cells on Matrigel-coated inserts to that on uncoated inserts. Experiments were performed in triplicate, and the means with standard deviations of the values are shown in the graphs in Fig. 8.

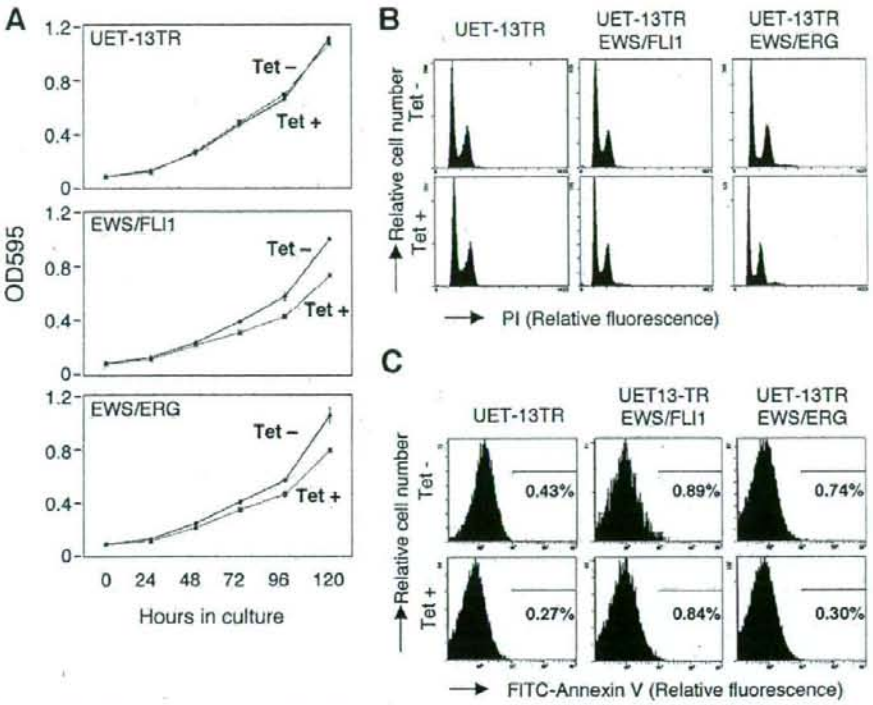

FIG. 2. Effects of EWS/ETS on cell growth in UET-13 cells. (A) Growth curve for UET-13 transfectants. Cells were seeded at 10^3/well and cultured as described for Fig. 1. The increase in cell number was analyzed by MTT assay. Values are means with the standard errors (SE) from three independent experiments. Diamond symbols indicate UET-13 transfectants in the absence of tetracycline (Tet); box symbols indicate UET-13 transfectants in the presence of tetracycline. (B) Cells were cultured as described for panel A in the absence or presence of tetracycline for 3 days and then stained with PI, and DNA contents were analyzed by flow cytometry (*x* axis, relative intensity of fluorescence; *y* axis, relative cell number). (C) Cells treated as described for panel B were stained with FITC-annexin V and analyzed.

Microarray data accession numbers. Microarray data have been deposited in the Gene Expression Omnibus database GEO (www.ncbi.nlm.nih.gov/geo) (accession numbers GSE8665 and GSE8596).

RESULTS

EWS/ETS expression results in morphological changes in UET-13 cells. To investigate how the expression of EWS/ETS affects human MPCs, we used UET-13 cells as a model of human MPCs and expressed EWS/FLI1 (UET-13TR-EWS/FLI1) and EWS/ERG (UET-13TR-EWS/ERG) in a tetracycline-inducible manner (Fig. 1A). As shown in Fig. 1B and C, we confirmed that the tetracycline treatment could induce EWS/ETS expression by RT-PCR analysis and Western blotting. The inducibility upon the addition of doxycycline was comparable to that upon the addition of tetracycline.

Using these cell systems, first we examined the effect of EWS/ETS expression on morphology in UET-13 transfectants. When tetracycline was added to the culture, the morphologies of both UET-13TR-EWS/FLI1 and UET-13TR-EWS/ERG cells were dramatically changed (Fig. 1D). Tetracycline-treated UET-13TR-EWS/ETS cells consisted of a mixture of small round-to-polygonal cells and short spindle cells. The cell morphology resembled that of EFT cell lines. To assess the reproducibility of this phenotypic change, other UET-13TR-EWS/ETS clones were examined, and similar morphological changes were observed. Since tetracycline treatment did not affect the morphology of UET-13TR cells (Fig. 1D), it was suggested that the morphological alteration in UET-13 cells from a mesenchymal cell shape to small round cells, one of the characteristics of EFT, can be attributed to EWS/ETS expression.

EWS/ETS expression inhibits cell growth in UET-13 cells. Next, the effect of EWS/ETS expression on the growth of UET-13 cells was analyzed. As shown in Fig. 2A, an MTT assay revealed that the addition of tetracycline had no effect on the growth of UET-13TR cells but slightly inhibited that of UET-13TR-EWS/ETS cells. We also assessed the cell growth of UET-13 transfectants after tetracycline addition by cell counting and obtained results well in accord with those from the MTT assay (data not shown). To determine the mechanism of this inhibition, DNA content and the binding of annexin V to UET-13 transfectants were examined. No significant increase in either sub-G_1-phase cells (Fig. 2B) or annexin V binding cells (Fig. 2C) was detected, suggesting that EWS/ETS-mediated growth inhibition in UET-13 cells was not due to the activation of an apoptotic pathway. Moreover, no significant decrease in S-G_2-phase cells was observed (Fig. 2B).